Role of $Na_V1.9$ in activity dependent axon growth in embryonic cultured motoneurons

Dissertation zur Erlangung des naturwissenschaftlichen Doktorgrades der Bayerischen Julius-Maximilians- Universität Würzburg

vorgelegt von
Narayan Subramanian,
aus Mumbai, Indien.

Würzburg, 2011

Eingereicht am:……..

Mitglieder der Promotionskommission:

Vorsitzender: Prof. Dr. Thomas Dandekar

Erstgutacher: Prof. Dr. Michael Sendtner

Zweitgutacher: Prof. Dr. Erich Buchner

Tag des Promotionskolloquiums:…….

Doktorurkunde ausgehändigt am:…….

Table of contents

1. Summary

Spontaneous neural activity has been shown to regulate crucial events in neurite growth including axonal branching and path finding. In animal models of spinal muscular atrophy (SMA) cultured embryonic mouse motoneurons show distinct defect in axon elongation and neural activity. This defect is governed by abnormal clustering of Ca^{2+} channels in the axonal regions and the protruding growth cone area. The mechanisms that regulate the opening of calcium channels in developing motoneurons are not yet clear.

The question was addressed by blocking neural activity in embryonic cultured motoneurons by pharmacological inhibition of voltage-gated sodium channels (VGSC) by saxitoxin (STX) and tetrodotoxin (TTX). Low dosages of STX resulted in significant reduction of axon growth and neural activity in cultured motoneurons. This pharmacological treatment did not affect survival of motoneurons in comparison to control motoneurons that was grown in the presence of survival neurotrophic factors BDNF and CNTF. It was also found that STX was 10 times more potent than TTX a common inhibitor of VGSC with a reduced activity on the TTX-insensitive sodium channels $Na_V1.5$, $Na_V1.8$ and $Na_V1.9$. Reverse Transcriptase-PCR experiments revealed the presence of $Na_V1.9$ as the likely candidate that begins to express from embryonic stage sixteen in the mouse spinal cord. Immunolabelling experiments showed that the channel is expressed in the axonal compartments and axonal growth cones in cultured motoneurons. Suppression of $Na_V1.9$ in cultured motoneurons by lentivirus mediated short hairpin-RNA (shRNA) resulted in shorter axon length in comparison with uninfected and scrambled constructs. Further, embryonic motoneurons cultured from $Na_V1.9$ knockout mice also showed a significant reduction in neural activity and axon growth.

The findings of this work highlight the role of $Na_V1.9$ as an important contender in regulating activity dependent axon growth in embryonic cultured motoneurons. $Na_V1.9$ could therefore be considered

as a prospective molecule that could play an important role in regulating axon growth in motoneuron disease models like spinal muscular atrophy (SMA).

2. Zusammenfassung

Spontane neuronale Aktivität reguliert essentielle Ereignisse im Neuritenwachstum, wie beispielsweise die axonale Verzweigung und die Erkennung des Wachstumspfades. Motoneurone, die aus Tiermodellen der Spinalen Muskelatrophie (SMA) gewonnen werden, zeigen einen auffälligen Defekt im Streckenwachstum von Axonen und in der neuronalen Aktivität. Dieser Defekt wird von anormaler Clusterbildung von Ca^{2+} Kanälen in axonalen Regionen und in Wachstumskegeln begleitet. Die Mechanismen, die das Öffnen von Kalziumkanälen in embryonalen Motoneuronen in der Entwicklung regulieren, und die für das aktivitätsabhängige Axonwachstum benötigt werden, sind nicht bekannt.

Diese Frage wurde in dieser Studie bearbeitet, indem neuronale Aktivität in embryonalen Motoneuronen durch pharmakologische Inhibition von spannungsabhängigen Natriumkanälen durch Saxitoxin (STX) und Tetrodotoxin blockiert wurde. Geringe Dosen von Saxitoxin bewirkten eine deutliche Reduktion des Axonwachstums und der neuronalen Aktivität in kultivierten Motoneuronen. Diese pharmakologische Behandlung beeinflusste nicht das Überleben von Motoneuronen im Vergleich zu Kontroll-Motoneuronen, die in der Anwesenheit der neurotrophen Faktoren BDNF und CNTF kultiviert wurden. Saxitoxin war etwa 5-10-mal potenter als TTX, ein üblicher Blocker spannungsabhängiger Natriumkanäle mit einer verminderte Aktivität auf die TTX-insensitiven Natriumkanäle $Na_V1.5$, $Na_V1.8$, und $Na_V1.9$. Reverse-Transkriptase-PCR Experimente bestätigten die Anwesenheit von $Na_V1.9$ am Tag E16 (embryonaler Tag 16) im Rückenmark der Maus. $Na_V1.9$ ist ein einzigartiger Typus von einem Natriumkanal welcher in der Lage ist neuronale Erregbarkeit in der Nähe des Ruhemembranpotentials zu steuern. Deshalb war $Na_V1.9$ ein guter Kandidat für einen Kanal, der spontane Erregung in Motoneuronen vermittelt. Immunofärbungen zeigten, dass $Na_V1.9$ in axonalen Kompartimenten und axonalen Wachstumskegeln von kultivierten Motoneuronen exprimiert ist. Die

Unterdrückung von $Na_V1.9$ in kultivierten Motoneuronen durch lentiviral-exprimierte *short hairpin*-RNA (shRNA) resultierte in kürzerer Axonlänge, im Vergleich zu nicht-infizierten Motoneuronen oder Motoneuronen, die eine sinnlose Kontroll-shRNA Sequenz exprimierten. Embryonale, kultivierte Motoneurone von $Na_V1.9$ *knockout* Mäusen zeigten eine signifikante Verringerung der neuronalen Aktivität und verkürzte Axone. Diese Ergebnisse weisen auf eine Bedeutung von $Na_V1.9$ im aktivitätsabhängigen Axonwachstum hin

3. Introduction

The mammalian neuromuscular system controls the regular movements of the skeletal muscles via motoneurons that innervate them. Upon stimulation the motoneurons release neurotransmitters targeting the post-synaptic receptors at the neuromuscular junction to activate the skeletal muscle. Motoneurons that find their path towards the skeletal muscles undergo series of differentiation and physiological cell death mechanisms before reaching their skeletal targets. (deLapeyriere and Henderson, 1997; Hamburger and Yip, 1984; Sanes and Lichtman, 1999) Those motoneurons that mature and reach their target are the ones that remain alive throughout the animal's life span. Any sort of deregulation in axonal pathfinding towards their target skeletal muscles, excessive motoneuron death or disorganization of motor axon endplates at the skeletal muscles, results in progressive motoneuron diseases (Murray et al., 2008). The occurrences of these progressive neuromuscular diseases are more prominent in humans either during early development or during the final stages of adulthood. Two of the known and extensively studied motoneuron diseases in humans include the spinal muscular atrophy (SMA) (Greensmith and Vrbova, 1997; Monani et al., 2000; Sendtner, 2001), and the Amyotrophic lateral sclerosis (ALS) (Boillee et al., 2006; Bruijn et al., 2004; Rosen et al., 1993). SMA is characterized by progressive muscle paralysis, motoneuron loss and degeneration of lower motor neurons (Monani et al., 2000), while ALS includes progressive paralysis and degenerative disorder of upper and lower motoneurons where in the disease process spreads from the lower to the upper motor neurons (Chou and Norris, 1993). Though the functional importance of motoneurons in these neuromuscular diseases have been have been extensively studied, their physiological susceptibility leading to defects in path-finding and cell-death has not given rise to clinical success towards the treatment of neuromuscular diseases(Schmidt et al., 2009). Characterizing the molecular basis and functional patho-

mechanisms involved in motoneuron growth and maturation in animal models of motoneuron diseases opens up new roads for therapeutic strategies that could be applied for counteracting these challenges (Beck et al., 2001; Schmidt et al., 2009).

3.1 Role of neurotrophic factors in motoneuron survival

Prolonged existence and maintenance of motoneurons are necessary for the development of the neuromuscular system. Very early experiments performed in the developing chick embryo have shown that significant population of motoneurons are eliminated after contacting their target muscle, through a process of physiological cell death, thus giving rise to the importance tropic support for motoneuron survival provided by the skeletal muscles. (Hamburger, 1975; Sendtner et al., 2000; Son and Winzer-Serhan, 2009). Further advances since then have identified neurotrophic factors from various gene families playing an important role in motoneuron survival, development, regeneration and maintenance in the skeletal muscle (Grumbles et al., 2009; Hughes and O'Leary, 1996; Sendtner et al., 2000). The important neurotrophic factors include factors from the neurotrophin (NT) family, glial derived neurotrophic factors (GDNF), ciliary neurotrophic factors (CNTF) from the Schwann cells, LIF (leukaemia inhibitory factor) and Insulin like growth factors I and II (IGF). These neurotrophic factors bind to their respective receptors that are expressed in skeletal muscles and thereby acting on neurons that innervate them (Lai and Ip, 2003). Of the above mentioned neurotrophic factors, the family of neurotrophins are important not only for promoting neuronal survival (Cui, 2006) but also for playing an important role in cell fate decisions, axon growth, dendritic arborisation, cell migration, cell proliferation and activity dependent developmental processes (Huang and Reichardt, 2001; Markus et al., 2002; Segal, 2003; Thoenen, 1995).

3.2 Neural activity in developing nervous system

The dependence of neural activity for the formation of synapse has been shown to be present in various stages of neuronal development (Mennerick and Zorumski, 2000). The developing phases of the nervous system involving proliferation of neural stem cells that give rise to large population of neurons, migration of these neural precursors and finally differentiation into mature neurons in order to reach their target are governed and regulated by neural activity (Spitzer, 2006; Webb et al., 2005). Embryonic neurons that differentiate to reach their muscle target possess the ability to generate spontaneous electrical activity. These forms of spontaneous activity are quite different from those generated by mature neurons in terms of their higher specificity to initiate and regulate various aspects of cellular development (Hanson et al., 2008). Because of this excitable nature of neurons, voltage-gated ion channels that are expressed at early stages of development play an important role in the regulation of neural activity (Moody and Bosma, 2005; Takahashi and Okamura, 1998),

3.3 Spontaneous neural activity in spinal motoneurons

Motoneuron morphogenesis includes axon outgrowth and guidance that is devised during embryonic development to establish the correct wiring within the neuromuscular system.Motoneurons find their path over long distances to innervate skeletal muscles at motor endplates (Hanson and Landmesser, 2006; Melancon et al., 1997), and thereby forming a synaptic network with other neurons. Although these initial synaptic connections are formed largely through molecular mechanisms that depend on intrinsic developmental programs, spontaneous and experience driven electrical activities play an important role in shaping the development of neuromuscular system. This spontaneous electrical activity is driven by voltage-gated ion channels

that are present at the motoneuron end plates thereby playing an important role in axon elongation and path finding (Hanson et al., 2008; Landmesser and O'Donovan, 1984), synapse maturation (Gonzalez-Islas and Wenner, 2006) and development of pattern generating circuits (Marder and Rehm, 2005; Myers et al., 2005). Spontaneous neural activity has been studied in detail in the developing neocortex, thalamus, hippocampus, retina and spinal cord by direct recording of electrical activity or fluorescence imaging of Ca^{2+} transients (Feller, 1999; O'Donovan et al., 1998). In general, this activity consists of synchronous or asynchronous bursts of action potentials that last for approximately between ten to hundreds of milliseconds, separated by intervals of a few minutes depicting a fire-pause-fire scenario. This kind of activity involves continuous firing of large populations of neurons or spontaneous localized activity from few cells in a population. The activity may also remain localized to discrete domains in the entire cell for example the growth cone, distal or proximal axons or the dendritic region in the cell body or perhaps the entire cell (Jablonka et al., 2007) as observed in regions like the neocortex (Yuste et al., 1992) and the spinal cord (O'Donovan et al., 1998) or may spread from one region to another in the form of propagating electrical waves, such as those observed in the developing retina (Meister et al., 1991).

In response to membrane depolarization, voltage-gated calcium channels (VGCC) mediate the entry of Ca^{2+} influx and thus regulate different intracellular processes. Changes in the intracellular Ca^{2+} concentration due to spontaneous or programmed signalling event have been shown to initiate important cellular events like differentiation of skeletal and heart muscles (Zheng and Poo, 2007). The role of Ca^{2+} is that of an intracellular secondary messenger that can mediate local and global responses in the same cell (Bootman et al., 2001). Electrical activity triggers an increase in intracellular Ca^{2+}concentration, which, by activating different signalling cascades. This in turn is responsible for

various developmental events including regulation of growth of axons and axonal guidance (Gomez and Zheng, 2006; Spitzer, 2006). Previous studies in Xenopus spinal neurons have indicated that during the time of closure of the neural tube, prior to synapse formation, voltage-gated ion channels are expressed, and that the collection of the channels expressed at this time allow Ca^{2+} influx (Spitzer and Ribera, 1998). Studies have also shown that removal of extracellular Ca^{2+} from the medium disturbed the differentiation of neurons in dissociated cell culture (Bixby and Spitzer, 1984; Desarmenien and Spitzer, 1991; Spitzer et al., 1993)]. Thus one of the aspects of motoneuron differentiation involves targeting of axons that extend to synapse with other neurons at the neuromuscular system.

3.4 Activity dependent axon growth in motoneurons

Embryonic motoneurons in culture exhibit spontaneous elevations of free intracellular Ca^{2+} concentration both in culture and in vivo during an early period of differentiation, as revealed by previous studies by imaging the fluorescence of Ca^{2+} indicator dyes. These spontaneous elevations can be eliminated by removal of extracellular Ca^{2+} or pharmacological application of pharmacological Ca^{2+} channel blockers like ω-conotoxin. (Gu et al., 1994; Gu and Spitzer, 1993; Holliday and Spitzer, 1990). In embryonic *Xenopus* spinal neurons, two types of Ca^{2+} transients have been characterized both *in vitro* and *in vivo*: fast-rising global Ca^{2+} spikes with characteristics of action potentials, and slower Ca^{2+} transients, termed waves, generated in the growth cone region (Gu et al., 1994). Interfering with either type of calcium transients results in suppression of neurotransmitter GABA, thereby enhancing neurite growth. Studies performed on cultured embryonic mouse motoneurons show the presence of localized spontaneous calcium transients at the growth cone and the somatodendritic compartment. These spontaneous calcium transients were severely abolished in the mouse model for spinal

muscular atrophy (SMA) (Jablonka, 2007). Isolated embryonic motoneurons from *Smn*$^{-/-}$*,SMN2* mice show reduced motor axon growth in culture and further show defects in the clustering of N-type voltage-gated calcium channel(VGCC) $Ca_V2.2$ in axon terminals. This clustering defect of $Ca_V2.2$ in axonal growth cones correlates with a reduced rate of local Ca^{2+} transients at distal axons and growth cones (Jablonka, 2007). It has been also shown that axon growth in cultured embryonic mouse motoneurons is supported by laminin-111, while other substrate compositions consisting of laminin211/221 reduce axon elongation (Jablonka et al., 2007). Pharmacological inhibition of N-type Ca^{2+} channels with ω-conotoxin in embryonic motoneurons cultured on laminin-111, results in reduced axon length, in a concentration dependent manner (Jablonka et al., 2007). The study also showed that these spontaneous calcium transients could be blocked by 1 μM TTX (TTX), indicating that they are triggered by opening of VGSC (VGSC).

Spontaneous electrical activity is also found in developing motoneurons before the formation of functional synapses at the neuromuscular endplates. During the development of spinal cord, motoneurons exhibit large periodic depolarizations that are separated by extended time points of resting states of silence, a pattern that is able to control the movements of embryonic limbs (Provine, 1972) . This spontaneous network activity is observed over an extended period of development, from before motor neurons innervate muscle fibres (Milner and Landmesser, 1999) until multiple circuits that are formed becomes functional towards late embryonic development (Yvert et al., 2004)

3.5 Objective of the work

In neuromuscular disease models of spinal muscular atrophy (SMA), motoneurons in culture show reduced axon growth. Previous studies by Jablonka *et al 2007* have shown that spontaneous calcium transients in axonal growth cones of cultured embryonic motoneurons correlate with axon elongation (Jablonka et al., 2007). Motoneurons deficient in the survival motoneuron (*smn*) gene exhibit severe defects in the clustering of voltage-gated $Ca_v2.2$ channels in axonal growth cones. These defects correlate with reduced frequency of local Ca^{2+} transients (Jablonka et al., 2007) in axons and axon terminals. The work presented here is focused to the question whether VGSC are mediators or even an upstream trigger of spontaneous activity in embryonic motoneurons. Another aim of this work was the molecular identification among the nine isoforms of VGSC, responsible for triggering spontaneous Ca^{2+} influx to cultured embryonic motoneurons.

4. Materials and Methods

4.1 Materials

4.1.I Laboratory Animals

All the laboratory animals were bred in the animal facility at the Institute of Clinical Neurobiology, Universität Würzburg, in accordance with applicable policies and under pathogen free conditions. They were maintained under 12h/12h day-night rhythmic with complete access to food and water. The animal rooms were controlled at 21±1℃ and 50-60% relative humidity.

4.1.II Cell lines

1. HEK293T cells
2. HELA cells

4.1.III Chemicals

Unless mentioned all the chemicals used in this study were of analytical grade and purchased from the following companies: Applichem, Amersham, Calbiochem, Chemicon, Fluka, Fermentas, Merck, Invitrogen, Sigma and Roth

4.1.IV Cell culture

❖ **Components for Motoneuron Culture**	**Source/ Company**
Neurobasal Medium	Invitrogen
Glutamax	GIBCO
Hank's Balanced Salt Solution (HBSS)	PAA
Horse Serum	Linaris
B-27 Supplement	GIBCO
Laminin	Invitrogen

Trypsin (1%)	Worthington
Trypsin Inhibitor (1%)	Sigma
Poly-D-Ornithine	Sigma
1X Phosphate Buffer Saline (PBS)	PAA
Tetrodotoxin (TTX)	Ascent Scientific
Saxitoxin (STX)	Ascent Scientific
BDNF	(Institute of Clinical Neurobiology, Uni-Wuerzburg)
CNTF	(Institute of Clinical Neurobiology, Uni-Wuerzburg)

❖ **Components for Lentivirus ProductionSource/Company**

OptiMEM	Invitrogen
DMEM (high glucose) +HEPES	Invitrogen
MEM	Invitrogen
Fetal Calf Serum	Linaris
Penicillin / Streptomycin	Invitrogen
DMSO	Sigma
Lipofectamine2000	Invitrogen
Glutamax	Life Technologies
Geneticin (G418)	Invitrogen

❖ **Components for 4% Paraformaldehyde solution (4% PFA)**

- 1.6g PFA
- 20ml Distilled water
- 3 dry pellets of NaOH
- Warmed in 60℃ water bath till PFA is dissolved.
- 16.4 ml Na_2HPO4 (0.2 M)
- 3.6 ml NaH_2PO4 (0.2M)
- pH 7.1 – 7.4

❖ **Preparation of Mowiol® 4-88 mounting agent. (Polysciences Europe GmbH)**

1. Mix using a magnetic stirrer,4.8g Mowiol® 4-88 and 12g glycerol (100ml beaker)
2. Add 12ml ddH2O and continue stirring till a clear solution is formed at room temperature.(at least 4 hrs)
3. Add 24ml 0.2 M Tris HCl (ph 8.5). Continue stirring. Heat occasionally to 50˚c in a water bath (10 min).
   Continue stirring until Mowiol is dissolved.
4. Spin down the solution at 500 x g for 15 minutes to get a clear solution at the top.
5. Preserve the supernatant and store aliquots at -20˚c.

4.1.V Live cell imaging reagents,

➢ **ACSF (Prepared in periodic batches of 5 litres and stored at 4°C)**

- 127 mM NaCl
- 3.0 mM KCl
- 1.25 mM NaH_2PO4 H_20
- 23.0 mM $NaHCO_3$
- 25.0 mM Glucose (added fresh on the day of performing Ca^{2+} imaging)

➢ **5 µM Oregon Green 488 BAPTA-1, AM- Invitrogen**

➢ **FURA-2 AM Invitrogen**

4.1.VI Buffers and Solutions

- **10mM Tris EDTA buffer (TE buffer) (1L)**
  - 10ml 1M Tris-HCl (pH 8.0)
  - 2 ml 500 mM EDTA (pH 8.0)

- **Mouse tail lysis buffer**
  - 0.1M Tris-HCl (pH 8.5)
  - 5mM EDTA (pH 8.0)
  - 0.2% SDS
  - 200mM NaCl

- **Annealing buffer:**
  - 100mM K-acetate
  - 30mM HEPES-KOH pH 7.4
  - 2mM Mg-acetate

- **Qiagen buffer 1**
  - 50 mM Tris HCl pH 8.0
  - 10 mM EDTA
  - 100 ug/ml RNase A
  - Stored at 2-8C after addition of RNase A

- **Qiagen buffer 2**
  - 200 nM NaOH
  - 1% SDS

- **Qiagen buffer 3**
  - 3 M Potassium acetate, pH 5.5

- **SOC medium**

  - SOB medium

    - 20g tryptone
    - 5g yeast extract
    - 0.58g NaCl
    - 0.19g KCl
    - 4ml 1M NaOH
    - dd H_2O to 1 litre and autoclave. Just before use add: 5ml 2M MgCl2 / L

  - For SOC 20 mM of filter sterile glucose is added to SOB

4.1.VII Kits

- 1st strand cDNA synthesis kit for RT-PCR (AMV) Roche
- NucleoSpin© Plasmid Machery & Nagel
- Big-Dye Terminator Mix Applied Biosystems
- QIAquick® gen Gel Extraction Kit Qiagen
- QIAquick® PCR Purification Kit Qiagen
- Endofree® Plasmid Maxi kit Qiagen

4.1.VIII Plasmids

	Vectors	Source
1.	pll3.7	Institute of Virology (Rubinson et al., 2003)
2.	pMD.G VSVG	Institut für Virologie, Würzburg (Dull et al., 1998)
3.	pRSV-REV	Institut für Virologie, Würzburg (Dull et al., 1998)
4.	pMDLg/pRRE	Institut für Virologie, Würzburg (Dull et al., 1998)
5.	pllshNa$_V$1.9	Self cloned in this work
6.	pllmisNa$_V$1.9	Self cloned in this work
7.	pSIHs63 (shNa$_V$1.9)	Cloned by PD. Dr. Robert Blum,
8.	pSIHm63 (misNa$_V$1.9)	Cloned by PD. Dr. Robert Blum,

Table 4.1. List of plasmids

4.1.IX Antibodies for Immunocytochemistry

❖ **Primary Antibodies:**

Sr. No:	Antibody	Host species	Company / Source	Dilution
1.	anti-Tau	Rabbit	Sigma	1:1000
2.	anti-βIII-Tubulin	Monoclonal, mouse	Developmental Studies Hybridoma Bank E7	1:1000
3.	anti-GFP	Chicken	Abcam	1:2000
4.	anti-$Na_V1.9$	Rabbit	T-71 (Robert Blum-Institute of Clinical Neurobiology-Würzburg)	1:100 (1:10 prediluted)
5.	anti-trkB	Monoclonal, mouse	Transduction	1/500-1/1000
6.	anti-RFP	Rabbit	Rockwell	1:2000

Table 4.2. List of primary antibodies

❖ **Secondary Antibodies:**

Sr.No	Antibody	Host species	Company/ Source	Dilution
1.	DyLight488 goat-anti-mouse IgG	mouse	Jackson Immuno	1/800-1/1600
2.	Cy 3 Goat Anti-Rabbit IgG (H+L)	Rabbit	Jackson Immuno	1/350
3.	DyLight488 goat-anti-rabbit IgG	Rabbit	Jackson Immuno	1/800
4.	FITC Mouse Anti- Chicken	Mouse	Jackson Immuno	1/800

Table 4.3. List of secondary antibodies

4.1.X Oligonucleotide Sequences

❖ Primers for cDNA amplification:

1. Scn8afwd 5’-GAA GAG GTA TCT GCA GTG GTC-3’
2. Scn8arev 5’-CTA GCA CTT GGA CTC CCT GAC-3’
3. Scn11afwd 5’-GGT GTT TTG CAA TGG AGA CTT GTC-3’
4. Scn11arev 5’-GAG CTA CAT GTG GCA GGT CAC ATA C-3’
5. Actin fwd: 5’-GTG GGC CGC CCT AGG CAC CAG-3’
6. Actin rev 5’-CTC TTT AAT GTC ACG CAC GAT TTC-3’

❖ Primers for genotyping

1. TrkB Sense 5´-TCG CGT AAA GAC GGA ACA TGA TCC-3´
2. TrkB wt 5´-AGA CCA TGA TGA GTG GGT CGC C-3´
3. TrkB ko 5´-GAT GTG GAA TGT GTG CGA GGC C-3´

❖ Oligos for shRNA.

- **sh $Na_v1.9$ knockdown constructs cloned in pLentilox3.7 with eGFP as the marker. (Synthesized from © Eurofins MWG Operon)**

1. **Antisense 5503MScn11a-shRNA top Strand 5'-3'**

   tGATTGAACGTCGGAACATGTTCAAGAGACATGTTCCGACGTTCAATCTTTTTTc

2. **Antisense 5503MScn11a-shRNA bottom Strand 5'-3'**

   tcgagAAAAAAGATTGAACGTCGGAACATGTCTCTTGAACATGTTCCGACGTTCAATCa

3. **Scrambled mm5503MScn11a-shRNA top Strand 5' 3'**

   tGATTCAACGACGGTACAAGTTCAAGAGACTTGTACCGTCGTTGAATCTTTTTTc

4. **Scrambled mm5503MScn11a-shRNA bottom Strand 5'-3'**

   tcgagAAAAAAGATTCAACGACGGTACAAGTCTCTTGAACTTGTACCGTCGTTGAATCa

- **ShNa$_V$1.9 knockdown constructs cloned in pSIH-H1 with tandem tomato as marker**

5. **Antisense 63MScn11a-shRNA top Strand 5'-3'**

gatccGGTACTATCCAGTGATCTTCCCTTCCTGTCAGAGGAAGATCACTGGATAGTACCttttg

6. **Antisense 63MScn11a-shRNA bottom Strand 5'-3'**

aattcaaaaaGGTACTATCCAGTGATCTTCCTCTGACAGGAAGGGAAGATCACTGGATAGTACCg

7. **Scrambled 63MScn11a-shRNA top Strand 5'-3'**

gatccGGTCTATTGACTAGCACTTCCCTTCCTGTCAGAGGAAGTGCTAGTCAATAGACCttttg

8. **Scrambled 63MScn11a-shRNA bottom Strand 5'-3'**

aattcaaaaaGGTCTATTGACTAGCACTTCCTCTGACAGGAAGGGAAGTGCTAGTCAATAGACCg

4.2 Methods

4.2.I Molecular Biology techniques

4.2.I.a Oligonucleotide design and shRNA cloning

In order to silence the gene encoding $Na_V1.9$, short oligonucleotide sequences were selected and cloned into the lentiviral vector Lentilox 3.7 (ATCC®Number: VRMC-39™). Target sequences that correspond to $AAGN_{18}TT$ were identified from the mRNA from the $Na_V1.9$ sequence with accession number NM_011887. The multiple cloning sites of Lentilox 3.7 are present immediately after the U6 promoter and contain an HpaI restriction site. Opening the vector with HpaI results in a blunt end prior to the -1 position in the U6 promoter. An XhoI restriction site is available downstream of the HpaI site. Thus the oligo was designed in such a way that there is a 5'T to reconstitute the -1 nucleotide of U6. The arrangement of the oligo was as follows:

Sense oligo: 5'T-(GN18)-(TTCAAGAGA)-(81NC)-TTTTTTC.

The antisense oligo represented the complementary sense oligo strand with additional nucleotides at the 5' end to generate the XhoI overhang. The loop sequence (TTCAAGAGA) was selected according to Brummelkamp et al., 2002

Cloning strategy

Oligo annealing protocol:

1 µl Sense oligo
1 µl Antisense oligo
48 µl Annealing Buffer

Incubate at 95° 4 minutes
70° 10 minutes.
Decrease temperature to 4° slowly (.1°C/min)
Incubate at 4° 10 min

4.2.I.bLinearization of the lentiviral vector

The Lentilox 3.7 vector was linearized with HpaI and XhoI. 3-5 μg of lentiviral vector was digested for 2 h with HpaI at 37°C. The linearized DNA was then purified by ethanol precipitation. The DNA pellet was dissolved in xx mM Tris EDTA (TE) buffer. HpaI cut linearized vector was then digested with the restriction enzyme XhoI for two hours at 37°C and again purified by ethanol precipitation. The final pellet was dissolved in Tris EDTA buffer and stored in -20°C.

4.2.I.c Ligation

The covalent linking of two DNA molecules was performed by T4 DNA ligase. The digested vector and the annealed oligos were taken in equimolar concentration of 1:1. The ligation was always carried out overnight at 16°C.

Component	Volume
Linearized Vector	x μl (equimolar concentration) Vector : Insert ratio 1:1 (molar ratio) (In this case 1ug Vector-7.0ng of annealed oligos
Annealed Oligo (Insert)	y μl (pmol/μl)
T4DNA Ligase	1 μl
10 X ligation buffer	2 μl
10mM ATP	1 μl
HPLC grade H_20	Adjusted to 20 μl.

Table 4.4. Ligation reaction for oligo cloning

4.2.I.dTransformation

The incorporation of foreign DNA into bacteria was efficiently achieved by using chemically competent E. coli bacterial cells from strains of HB101 or STBL2 cells (Invitrogen). For amplifying vectors, 10-100 pg of plasmid DNA were utilized for HB101 competent cells. For oligo cloning purposes 10 µl of the ligation reaction was used along with commercially purchased STBL2 competent cells. The competent cells were first thawed on ice. The plasmid DNA or the ligated DNA was then mixed with the competent cells by gentle tapping of the tube. The mixture was then incubated on ice for 30 minutes. Subsequently, the tubes were heat-shocked in a 42°C water-bath for 90 seconds. The tubes were then put on ice for one minute. To recover the cells from heat shock 1ml of sterile LB medium was added to the competent cells and then tubes were placed in a bacterial shaker at 30°C (for lentiviral constructs) for one hour. After incubation, 10% of the transformed bacterial cells were streaked on LB agar plates. These agar plates were then incubated overnight at 30°C instead of 37°C to prevent recombination events. For amplification of vectors, corresponding clones were grown at 37°C. For analysis of positive clones, single colonies were picked up from LB Agar plates and added to 4-5 ml of LB broth in 15 ml Falcon tubes and grown on 30°C for overnight (approximately 16 hours). Plasmid DNA was extracted from these clones by alkaline lysis method (4.2.I.e). For isolating highly pure and large amounts of plasmid DNA, steps mentioned in the cesium chloride purification method were followed (4.2.I.f).

4.2.I.eExtraction of plasmid DNA by alkaline lysis

The isolation of plasmid DNA from small quantities of LB broth was performed according to Birnboim and Doly, 1979 . The overnight bacterial culture was transferred to a 1.5 or 2.0 ml eppendorf tube. The culture was then centrifuged down by using a table top centrifuge at 4000 x g for 30 seconds. The supernatant was then carefully aspirated using vacuum suction without disturbing the pellet. To this pellet, 100 µl of Qiagen buffer 1 was added and then the pellet was thoroughly mixed so that no clumps remain at the end of mixing. After mixing the pellet to Solution I, 200 µl of Qiagen buffer 2 was added and repeatedly inverted 10-12 times to denature the mixture. The suspension forms a clear, viscous and a sticky solution. To this mixture, 150 µl of ice cold Solution III was added. The tube was incubated on ice for 5 minutes. Further on, the mixture was centrifuged at 12000 x g for 5 minutes at 4°C to separate the pellet containing proteins and the DNA at the supernatant. At the end of centrifugation the supernatant was removed carefully with a pipette and transferred to a fresh eppendorf tube. To this 900 µl of ice cold absolute ethanol (100%) was added. The DNA was then separated by centrifuging the mixture at 12000 x g for 5 min at 4°C. The pellet that contained the plasmid DNA was washed in 1 ml of ice cold 70% ethanol. The mixture was again centrifuged at 12000 x g for 5 minutes at 4°C. The supernatant was aspirated carefully and the pellet was air-dried at room temperature. The isolated pellet was dissolved in 50 -100 µl of TE buffer. The concentration of the DNA was measured by using a spectrophotometer (Nanodrop).

4.2.I.f Isolation of large quantities of plasmid DNA, cesium chloride (CsCl) method:

For knockdown experiments using the lentivirus based gene silencing strategy, high purity of plasmid DNA was achieved by utilizing the cesium chloride isolation protocol. The method involves seven major steps: (1) Inoculation of bacteria carrying the plasmid DNA of interest, (2) Isolation of crude DNA (alkaline lysis and ethanol precipitation), (3) Phenol chloroform purification of the DNA, (4) Ultracentrifugation, (5) Isolation of DNA-EtBr band, (6) Removal of ethidium bromide (EtBr), (7) Final Precipitation of pure plasmid DNA.

(1) Inoculation of bacteria:

A small inoculum from a freshly growing bacterial plate (LB) was taken and inoculated on a warm LB broth of 100-250 ml volume. The inoculated broth was incubated at 30°C and placed on a bacterial shaker at a speed of 150-170 rpm for a period of 18-20 hours.

(2) Isolation of crude DNA:

The growing bacterial culture was harvested by spinning down at 5000 x g for 20 minutes at 4°C. The pellet was completely re-suspended in 20 ml of Qiagen buffer 1 with RNase (100 µg/ml). To this re-suspended bacterial solution 20 µl of 10 mg/ml lysozyme, was added and incubated for 5 min at room temp. An equal volume of Qiagen Buffer 2 was poured immediately to this solution and incubated for 5 minutes with moderate shaking at small intervals of 1 minute each. At the end of 5 minutes, 20 ml of Qiagen Buffer 3 was added in order to precipitate the proteins. The mixture was allowed to stand on ice for minimum of 10 minutes and then filtered through a folded Whatman filter paper (18 cm, type-102, Hartenstein) pre-wetted with distilled water. To the clear filtrate, equal volume of isopropanol was added. The tubes were now centrifuged at 8000 x g for 1 hour at 4^{o}C. The supernatant was

aspirated and the pellet was then washed with 15 ml of ice cold 70% ethanol. This step removed the residual acid from Buffer 3. The tube was again centrifuged at the same speed of 8000 x g for 1 hour at 4^{o}C. The 70% ethanol was removed completely by aspiration and the tube was left to thoroughly air-dry at room temperature. The dry pellet was then dissolved in 15 ml of TE buffer pH-8.0.

(3) Phenol chloroform purification:

The plasmid DNA that was dissolved in TE was now treated with 7.5 ml of TE-equilibrated phenol and 7.5 ml of chloroform. The DNA-phenol-chloroform mixture was mixed and then centrifuged at 1500 x g at room temperature for 20 minutes in a swing out rotor. The upper aqueous phase (15 ml) was transferred to a fresh tube to which 1/10th volume (1.5 ml) of 3.5 M sodium acetate pH 5.2 was added and mixed well. The content of the tube was then centrifuged at 8000 x g for 1 hour at 4^{o}C. The supernatant was aspirated carefully and the pellet was washed with ice cold 70% ethanol by spinning again 8000 x g for 20 minutes at 4^{o}C. The supernatant was aspirated and the pellet was air-dried at room temperature and stored at -20^{o}C till further processing.

(4) Ultracentrifugation:

The reagents and materials required for ultracentrifugation are prepared one day before the beginning of the process. For each plasmid DNA, 8.8 g CsCl was stored in air tight 50 ml falcon tubes at room temperature. A fresh saturated solution of 10mg/ml ethidium bromide (EtBr) was dissolved in TE. On the day of performing the ultracentrifugation, the DNA pellets from step 3 were solved in 8.0 ml of TE buffer. This solution was added to the tube containing 8.8 g of CsCl. To this tube 800 µl of 10 mg/ml EtBr was added and mixed thoroughly. To avoid precipitates, the tube was placed in 37^{o}C water-bath for 15 minutes. The tubes were spun at full speed on a swing out rotor for 10

minutes at room temperature. The supernatant was removed and transferred to an optiseal tube (5/8 x 2 ¾ in., Beckman). The tubes were balanced accurately, sealed and transferred to a NVT rotor that has been placed at room temperature the previous day. The ultracentrifugation was performed at 65000 rpm for a period of 5 hours and 30 minutes at 20 ^{o}C along with maximum acceleration and slow brake settings.

(5) Isolation of DNA-EtBr band:

After ultracentrifugation, the tube was placed on a rack meant for optiseal tubes. A grey needle of 21 gauges was pierced on the top of the tube to assist ventilation. The tube was now placed on a stand in front of a UV lamp (365nm). When the UV lamp was lit, the lower band representing the supercoiled plasmid DNA was selected. Entire contents of the lower band was taken out using a 2ml syringe and collected on a new 15 ml falcon tube. The contents of the tube are either processed the same day or stored at room temperature for EtBr removal the following day.

(6) Removal of EtBr:

The removal of EtBr from DNA was performed by organic extraction under a chemical hood. A 2 ml volume of the buffer TE saturated with n-Butanol was mixed with DNA-EtBr solution. The contents were mixed thoroughly and centrifuged at full speed for 2 minutes on a swing out rotor. The upper organic phase containing Butanol and EtBr was discarded on a special EtBr waste disposal container. The EtBr extraction procedure was performed until and unless the upper organic phase was colourless. To remove any residual Butanol in the solution, an equal volume of diethyl ether was added at the last step. The upper organic phase containing the Butanol+ether was discarded. The residual ether was evaporated due to its volatile nature.

(7) Final Precipitation of pure plasmid DNA:

The residual DNA after EtBr removal was mixed with 2 volumes of TE. To this, 1/10 volume of 3M sodium acetate was added along with ice cold 100% ethanol. The mixture was mixed well and placed for more than 1 hour on ice or overnight at 4°C. The following day, contents of the tube are centrifuged at 10000 x g for 1 hour at 4°C. The supernatant was aspirated and the colourless pellet was washed with ice cold 70% ethanol. The content of the tube was centrifuged for 10 minutes at 10000 x g at 4°C. The supernatant containing ethanol was discarded by aspiration. The pellet was left for drying under a sterile laminar air-flow. In order to keep the DNA sterile, all further steps are done in aseptic conditions. To the dried pellet, 100-200 µl of sterile Tris Buffer of pH 8.0 was added. The DNA was aliquoted in smaller volumes for future packaging or transfection experiments.

4.2.I.g Isolation of total RNA

The isolation of total RNA from spinal cord tissues was performed by using TRIzol Reagent. Dissected tissues were put in a sterile RNase free reaction tube and directly frozen in liquid nitrogen. For long term storage, tubes were preserved at -80°C. On the day of total RNA preparation, 1ml of TRIzol reagent was added to per 50 to 100 mg of frozen tissues and homogenized either mechanically by a tissue homogenizer or by using *SilentCrusher* (Heidolph) instrument. The homogenized tissue was incubated at room temperature for 5 minutes. 200 µl of chloroform was added, thoroughly mixed by shaking vigorously for 15 seconds. The mixture was incubated at room temperature for 3 minutes. The tube was centrifuged at 12000 x g at 4°C for 15 minutes to separate the organic phases. After centrifugation, the upper clear aqueous layer was transferred to a fresh eppendorf tube. The precipitation of RNA was achieved by the addition of 0.5 ml of isopropanol. The contents of the tube were now incubated for 10 minutes at room temperature. The tube was centrifuged at 12000 x g for 15 minutes at 4°C to pellet the RNA. The pellet was washed with 1 ml of 70% DEPC-ethanol. The contents were again centrifuged at 12000 x g for 10 minutes at 4°C and the pellet was dried. The pellet was finally dissolved in 50 µl of DEPC treated RNase free water. The RNA concentration was then measured by a spectrophotometer (Nanodrop; Peqlab) at 260 nm.

4.2.I.h Reverse Transcriptase Polymerase Chain Reaction

To know the time of expression of $Na_V1.9$, Reverse transcription polymerase chain reaction (RT-PCR) was undertaken. The total RNA isolated by using the TRIzol reagent was used as the starting material to prepare cDNA by the enzyme reverse transcriptase. This cDNA was used as a template for conducting the PCR reactions by using $Na_V1.9$ specific primers. For the synthesis of cDNA and the subsequent PCR reactions, the RT-PCR kit from Roche, namely, 1st Strand cDNA Synthesis Kit for RT-PCR (AMV) was used. The procedures involving the preparation of cDNA from the total RNA are summarized in tabular formats presented below.

Synthesis of cDNA

Reagent	Volume /1 sample	Final conc^{n}.
10 x Reaction Buffer	2.0 µl	1x
MgCl2 [25 mM]	4,0 µl	5 mM
Primer, random hexamer	2.0 µl	0,08 A260 Units
dNTP-Mix	2.0 µl	1 mM
RNase Inhibitor	1,0 µl	50 Units
AMV Reverse Transcriptase	0.8 µl	≥ 20 Units
Total RNA	variable	
dd H_2O HPLC grade	variable	
Total volume	**20 µl**	

Table 4.5. cDNA synthesis from total RNA

The reagents for cDNA synthesis were added according to the above table. The reaction mixture was then incubated at the following temperatures for carrying out the reverse transcription.

❖ **Incubation conditions for Reverse transcription:**

	Temperature	Incubation duration (minutes)
Primer Annealing	25°C	10
Reverse Transcription	42°C	60
Enzyme Denaturation	95°C	10
Long term storage	4°C	∞

Table 4.6. Incubation steps for cDNA synthesis from total RNA from tissues.

❖ **RT-PCR reaction Mixture:**

Reagent	Volume (µl)	Final Concentration
10 X Taq Buffer (15 mM $MgCl_2$)	5	1 x (1.5 mM $MgCl_2$)
Taq DNA Polymerase (5 units /µl)	0.4	2 units / reaction.
dNTP Mix (10 mM)	1	0.2 mM
Forward primer 10 µM	1	0.2 µM
Reverse primer 10 µM	1	0.2 µM
Betain (5M)	10	1 M
Template cDNA	2	
HPLC H_20	29	
Total volume	**50**	

Table 4.7. RT-PCR reagents for investigating $Na_V1.9$ expression.

❖ **RT-PCR program conditions:**

Process	Temperature (°C)	Time	Cycles
Initial denaturation	94	10 minutes	
Denaturation	94	30 seconds	35 cycles
Annealing	52	30 seconds	
Primer Elongation	72	60 seconds	
Final Elongation	72	7 minutes	
Final storage	4	∞	

Table 4.8. PCR program to investigate $Na_V1.9$ expression.

4.2.II Cell Culture

4.2.II.a Motoneuron Culture

The technique of dissecting out lumbar spinal cord and preparing a motoneuron culture was performed according to Wiese et al., 2010 . To isolate spinal motoneurons, pregnant mice with fourteen day old embryos were sacrificed by cervical dislocation. Lumbar-spinal cords were isolated from the embryos and preserved in ice cold HBSS solution. For subsequent genotyping of embryos, the tail was dissected and placed in 400 µl of lysis buffer. Isolated spinal cords were trypsinized by the addition of 20 µl of 1% trypsin solution to each Eppendorf tube containing a dissected spinal cord in 180 µl ice-cold HBSS. Trypsinization was performed for 15 min at 37 ℃. To stop the process of trypsinization, 20µl of 1% trypsin inhibitor was added to the eppendorf tubes and then the tissue aggregates were mechanically triturated. The cells were now enriched from the triturated cells on a 10 cm panning plate that was previously coated with an antibody against the $p75^{NTR}$ receptor (1.8 mg/ml). The cells were placed on the panning dish and allowed to settle down for a period of 35 minutes after which they were washed thrice with room temperature warm Neurobasal medium in order to eliminate the $p75^{NTR}$ negative cells. The settled cells were depolarized with 30mM potassium chloride and then added to Neurobasal medium containing B27 supplement and 10% heat inactivated horse serum. Cells were counted on haemocytometer and plated at a density of 1500-2000 cells/coverslips for neurite length measurements and 25,000 cells on 12 mm coverslips for calcium imaging experiments. The neurotrophic factors BDNF and CNTF were added to the medium at a final concentration of 10 ng/ml. Pharmacological agents for sodium channel inhibitors STX and TTX were used at indicated concentrations. Motoneurons were treated with fresh medium within 24 hours after plating and further on after every alternate day till day seven.

4.2.II.b Immunocytochemistry

The technique of immunolabelling was utilized to analyse localization of proteins and neurite length measurements. Motoneurons that were isolated and cultured from mice of embryonic day 14 were allowed to grow for a maximal period of seven days. On the seventh day, the culture medium was aspirated using a Pasteur pipette and 1.5 ml of pre-warmed 4% paraformaldehyde was added for 15 min at room temperature. The cells were then washed three times with 1X PBS pH 7.0 at regular intervals of 10 minutes. Nonspecific binding sites were blocked for 1 hr with 1X PBS containing 15% goat serum and 0.3% Triton X-100. Cells were incubated at 4℃ over night (16 hrs) with primary antibodies. The following day, the primary antibodies were removed by aspiration or by pipette for future storages. The cells were immediately washed with 1xPBS, three to four times for at least one hour at room temperature. During the final washing steps fluorescently labelled secondary antibodies were diluted in blocking solution. At the end of the final primary antibody wash, 70 µl of diluted secondary antibody was added onto coverslips for a period of 1.5 hours. Secondary antibodies were then washed thoroughly by adding 1x PBS at periodic intervals of 2 minutes each. The secondary washes were performed for a period of 1 hour. Coverslips were then dipped in clean sterile water before mounting on mowiol or polymount on glass slides. These glass slides were then stored on slide boxes /slide folders, safely protected from light.

4.2.III Microscopy

4.2.III.a Neurite length measurements

Motoneurons labelled with anti-rabbit Tau or anti-mouse β-tubulin, was used as markers for staining axons and dendrites. For knockdown experiments, motoneurons infected with the respective knockdown or control (missense) lentivirus were labelled with either anti chicken GFP or anti chicken RFP marker to distinguish between infected and uninfected cells. Images were captured and analyzed on Leica TCS SP2 - Laser Scanning Spectral Confocal Microscope. Axon length was determined by applying a morphometric system (Leica, Bensheim, Germany). Values from at least three independent experiments were pooled, and the results were expressed as standard error of mean ± SEM.

4.2.III.b Motoneuron survival analysis.

To carry out motoneuron survival analysis the plastic surfaces of Greiner four well dish or the Nunc$^{\Delta}$ four well plates were first coated with poly-ornithine and laminin as described for motoneuron culture protocol. A plus sign was drawn at the bottom of each well thereby dividing the well into four equal quadrants. Cells were plated at a density of 5000 cells per 10mm diameter. Four to six hours after plating, motoneurons were counted using the phase contrast microscope, within an area of 1 μm from each marked quadrant. The same counting procedure was repeated at the end of day seven. Percentage survival was calculated on the basis of results obtained at the end of day seven.

4.2.III.c Ca^{+2} Imaging

Ca^{2+} imaging using Fura-2 AM dye (Jablonka et al., 2007).

Motoneurons grown till day three on glass coverslips were washed with phenol red free HBSS with Ca^{2+} & Mg^{2+} (5 min) and later on they were permeabilized with 0.25% pluronic F-127. Dye loading was performed by incubating 2µM FURA-2 for 30 minutes at 37°C. The coverslips were then transferred on a microscopic stage maintained at 37°C. HBSS with Ca^{2+} & Mg^{2+} was constantly perfused under linear flow. Upon calcium binding, the fluorescent excitation maximum of the indicator undergoes a blue shift from 363 nm (Ca^{2+}-free) to 335 nm (Ca^{2+} -saturated), while the fluorescence emission maximum is relatively unchanged at ~510 nm. The indicator was typically excited at 340 nm and 380 nm respectively and the ratio of the fluorescent intensities corresponding to the two excitations was used in calculating the intracellular concentrations. Florescent intensities that alternate after 340 nm or 380 nm stimulations were estimated by a computer overlay technique by selecting the region of interests (ROI) and thus calculate the bound and the unbound calcium. Live imaging of Ca^{2+} was undertaken by using an inverted microscope (Axiovert S100TV; Carl Zeiss MicroImaging, Inc.) equipped for epifluorescence with a dichroid mirror, a 100× 1.3 oil-immersion objective (Fluor; Carl Zeiss MicroImaging, Inc.), and a charge-coupled device camera (IMAGO; TILL Photonics).

Ca^{+2} imaging using Oregon green 488-BAPTA-1,AM

A 5 mM stock solution of Oregon green 488-BAPTA1, AM- a high affinity intracellular calcium indicator was used. The 5mM stock solution of Oregon-BAPTA1, AM was prepared by adding 8.9µl of 20% pluronic F-127 in DMSO. The mixture was dissolved by means of a sonifier bath for a period of 2 minutes. Motoneurons cultured on glass coverslips were transferred on 500 µl of 5mM Oregon-BAPTA1, AM in artificial

cerebrospinal fluid (ACSF) solution. The cells were then incubated in a cell culture incubator (37°C, 5% CO_2) for 15 minutes. The coverslips with dye- loaded cells were then transferred to the imaging set-up, wherein cells were imaged at 33-35°C using a 20X/0.7 objective under continuous ACSF perfusion. Pharmacological agents were used at the following concentrations: TTX at 10 nM, 100 nM and STX at 10 nM. During the continuous perfusion, time lapse imaging of Ca^{+2} dynamics was performed at 2.0 Hz/sec. Oregon Green-derived fluorescence was excited with a 488 nm laser line (emission filter: band pass 510/540 nm) and the live imaging of Ca^{2+} was performed in a inverted Leica TCS SP5 II confocal microscope.

4.2.IV Lentivirus Production

The lentiviral expression/knockdown system has been originated from the human immunodeficiency virus type 1 (HIV-1) and consist of the following three vectors:

- a packaging vector expressing the structural Gag and Gag-Pol proteins as well as regulatory and most of the viral accessory proteins;
- an envelope vector expressing heterologous surface glycoproteins —G glycoproteins of vesicular stomatitis virus (VSV-G); and
- a transfer vector containing human cytomegalovirus (CMV) promoter for heterologous protein expression (Naldini et al., 1996).

The bio-safety guideline of the system has been greatly improved by deletion of all accessory genes from the packaging vector (Dull et al., 1998).The viral packaging was performed by three helper packaging system as per the flowchart described in Figure 8. HEK 293T cells were co-transfected with lentiviral vector containing the knockdown or scrambled $Na_V1.9$, helper plasmids pRRE and pRSV (Dull et al., 1998) and the envelope expression plasmid pMD.G-VSVG that contains the vesicular stomatitis virus G glycoprotein (VSV-G) gene (Burns et al., 1993). Transfection was achieved by lipofectamine reagent that provides high transfection efficiency. The plasmid DNA and the lentiviral vector used in this lentiviral packaging were kept at highest possible purity by cesium chloride purifications (explained in 4.2.I.g). The knockdown lentivirus was finally dissolved in a Tris buffer solution and preserved in smaller aliquots of 10 µl each at -80°C for long term storage (Figure 4.1).

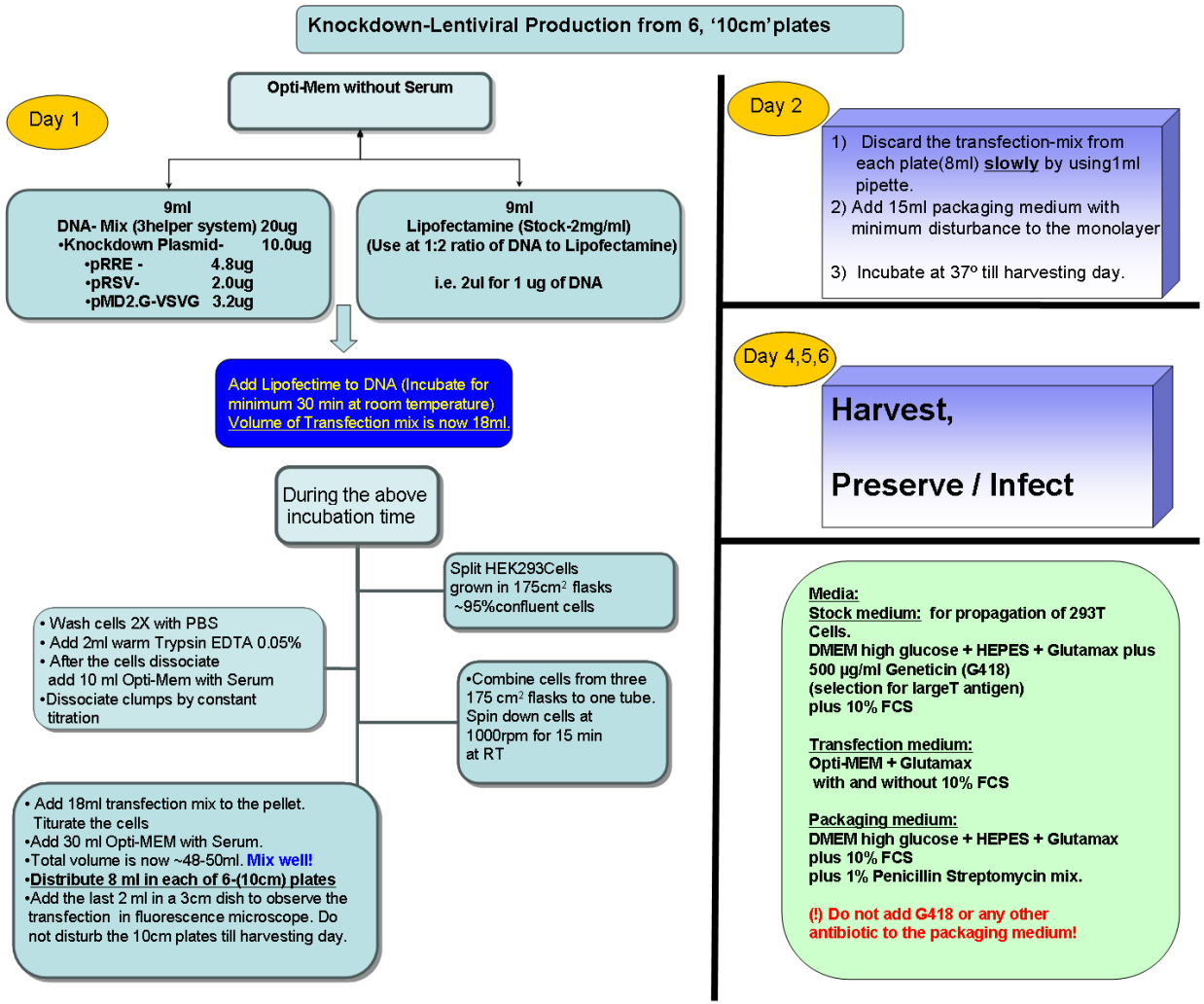

Figure 4.1 Flow chart for generation of shRNA knockdown lentivirus.

5. Results

5.1. Inhibitors of VGSC reduce axon growth of cultured embryonic motoneurons

Earlier studies from our group showed that local spontaneous excitability in axonal growth cones of cultured embryonic motoneurons correlates with axon elongation (Jablonka et al., 2007). We therefore asked whether VGSC are triggering spontaneous Ca^{2+} transients in motoneurons. In order to investigate this, mouse motoneurons were isolated from lumbar spinal cords at embryonic day (E) 14 and cultured for a period of seven days in the presence of survival neurotrophic factors BDNF and CNTF (10ng/ml) and in the presence of 100 nM STX, a potent blocker of all VGSC. At DIV7, motoneurons were fixed and immuno-labelled with α-Tau antibody and the axon length was measured. As shown in the Figure 5.1, motoneurons grown in 100 nM STX showed in significant reduction in axon length.

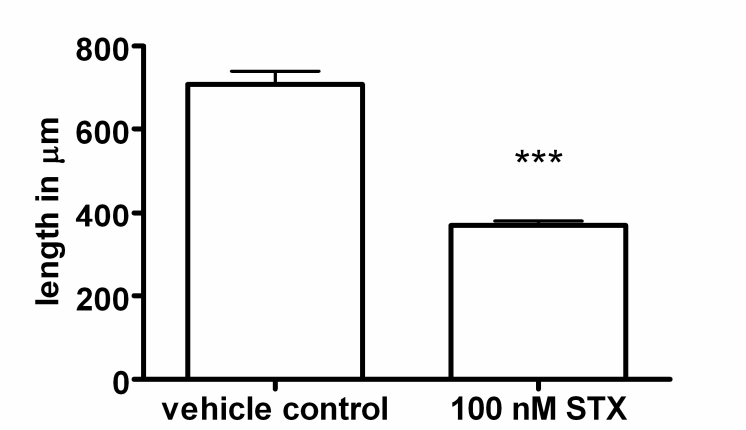

Figure 5.1 Axon length is reduced on the inhibition of VGSC with 100 nM (STX) in wild type motoneurons. Axon length is significantly reduced in STX treated motoneurons (n=215) in comparison to untreated (vehicle control n=121) motoneurons. Results represent the mean ± SEM of pooled data from three independent experiments. n, number of motoneurons that were scored in total from control or 100 nM STX treated cells.***,P<0.0001 tested by unpaired t test.

5.2. Inhibitors of VGSC reduce spontaneous Ca^{2+} elevation in cultured motoneurons.

In cultured embryonic motoneurons, the monitoring of spontaneous Ca^{2+} elevation is an appropriate tool to analyse motoneuron excitability (Jablonka et al., 2007) In order to analyse whether neural activity is affected on inhibition of VGSC, we further compared frequency of spontaneous calcium transients in cultured motoneurons in the presence and absence of sodium channel blockers STX (100 nM) and TTX (TTX) (1µM). Motoneurons were grown in these pharmacological conditions with regular medium exchanges on alternate days after day one. On day three motoneurons grown in the presence of STX and TTX were treated with calcium indicator dye Fura-2 and cytosolic increase of Ca^{2+} was measured at the growth cone and the somato-dendritic compartment (Jablonka et al., 2007).

In comparison with motoneurons treated with vehicle control 0.03N acetic acid, on day three motoneurons that were treated with 1µM TTX showed significant reduction in the frequency of calcium transients at the somatodendritic region as well as at the growth cone (Figure 5.2). Cellular excitability was further drastically reduced in the case of motoneurons treated with 100 nM STX on day three (Figure 5.2). Thus pharmacological treatment of sodium channel inhibitors STX and TTX results in severe reduction in cellular excitability on cultured motoneurons at the somato-dendritic compartment as well as the growth cone.

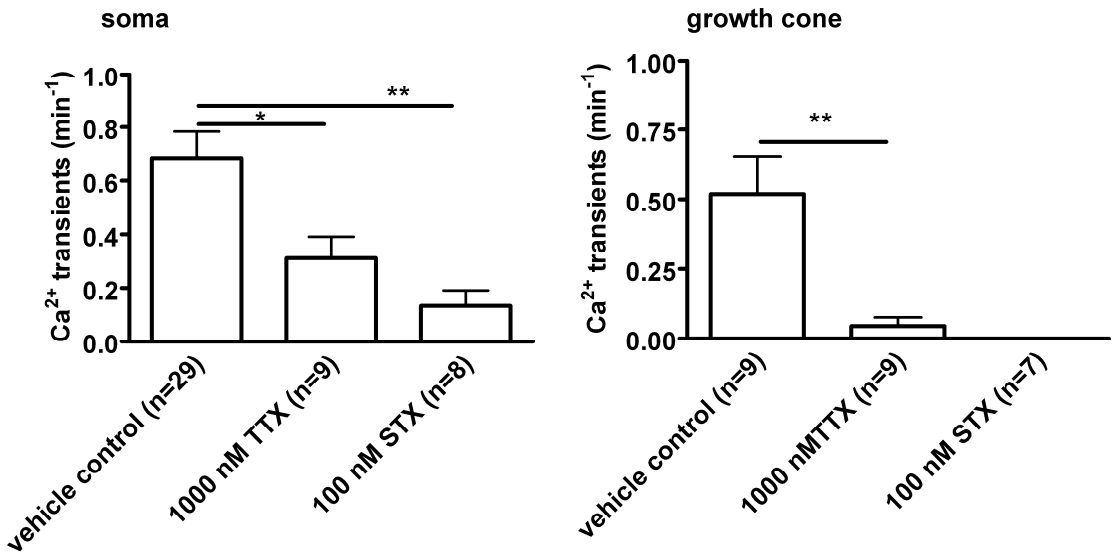

Figure 5.2 Frequency of calcium influx in the presence of STX and TTX is reduced in DIV3 embryonic cultured motoneurons. Results represent the mean ± SEM of pooled data from three independent experiments. n, number of motoneurons that were scored in total from control, 1µM TTX or 100 nM STX, treated cells.***,P<0.0001 tested by unpaired t test, one tailed.

In subsequent work by Benjamin Dombert in our institute, a dose-dependency curve was performed. In these experiments, motoneurons were cultured for seven days in the presence of the sodium channel blockers TTX at concentrations of 10 nM, 50 nM and 100 nM and STX at concentrations of 1 nM, 5 nM and 10 nM. These experiments revealed that motoneurons treated with 10 nM to 1 nM STX showed a significant decrease in axon length. Compared to STX, TTX was less effective. No reduction in axon elongation was observed under chronic treatment with 10nM TTX, but was obvious with 50 nM TTX (Subramanian et al., manuscript submitted). Thus lower dosages of pharmacological inhibitors of VGSC are able to reduce axon growth.

5.3. Survival tests for motoneurons under pharmacological treatments

Previous studies have shown that inhibition of VGSC results in 50% loss of developing retinal ganglion cells in culture (Lipton, 1986). Thus in order to rule out toxic effects of pharmacological sodium channel blockers, cultured motoneurons that were treated with varying dosages of STX and TTX were tested for their survival until DIV7. Motoneurons were grown in the presence of neurotrophic factors BDNF and CNTF at 10 ng/ml. Concentrations of TTX were at 10 nM, 50 nM and 100 nM, whereas of STX were 1 nM, 5 nM and 10 nM. As a negative control, motoneurons were grown in the absence of the above neurotrophic factors. Cells were counted on the day of plating and finally on day seven. Percentage survival of originally plated cells was compared under varying pharmacological conditions. Neither did the presence of STX nor TTX, resulted in reduced motoneuron survival (Figure 5.3), even not at concentrations showing drastic reduction in axon length. This experiment separates the growth-supporting signalling of various isoforms of sodium channels from signalling pathways for motoneuron survival.

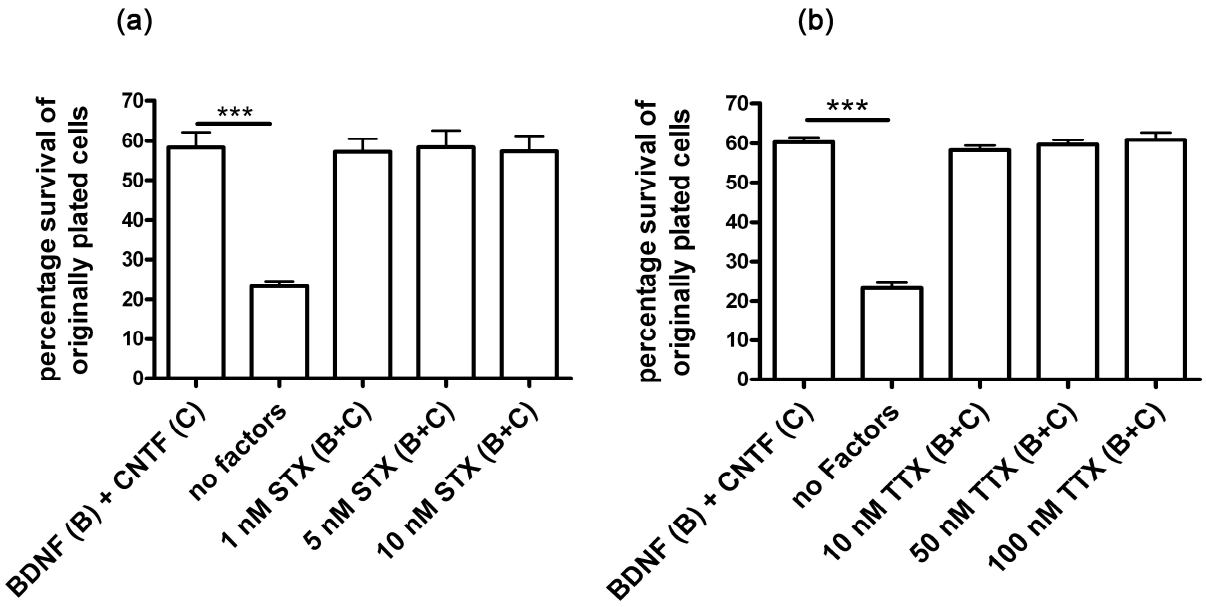

Figure 5.3 Survival of motoneurons is not affected by sodium channel inhibitors STX and TTX. Motoneurons were plated at a density of 5000 cells / well, and survival was determined after 7 d in culture. Survival rates of motoneurons treated with varying concentrations of (a) STX and (b) TTX were comparable to untreated cells. Results represent the mean ± SEM of pooled data from three independent experiments. ***, $P<0.0001$ tested by one-way ANOVA.

5.4. Pharmacological assay to analyze the role of VGSC in spontaneous Ca^{2+} elevation

Embryonic mouse motoneurons cultured in the presence of 1 µm TTX and 100 nM STX showed significant reduction in the frequency of calcium transients in comparison to vehicle controls. Since STX and TTX are known to be potential high affinity sodium channel blockers, it was needed to find out the minimal concentration of pharmacological toxins that was able to show a reduction in spontaneous motoneuron excitation. We therefore asked if acute treatment of STX or TTX is able to inhibit VGSC. For this it was essential to screen and visualize for cultured motoneurons that were spontaneously active when treated with a high affinity calcium indicator. For this purpose, we chose to utilize Oregon green BAPTA-1, and confocal Ca^{+2} imaging that provides an advantage of visualizing spontaneous calcium transients at higher frequencies. On performing live imaging of three day old cultured embryonic motoneurons for spontaneous calcium transients one could visualize different patterns of calcium transients which could be categorized according to the level of synchronicity. Cultured motoneurons exhibiting spontaneous Ca^{2+} transients could be as described below (Figure 5.4):

Type-1: low amplitude and countable calcium transients ,

Type-2: relatively greater amplitude size than type-1

Type3: no calcium transients at all

Type4: very high number of Ca^{2+} transients than those seen in Type-2 and those which were difficult to count.

Motoneurons that showed Ca^{2+} transients according to type 1 and 2 were utilized for pharmacological assays described further.

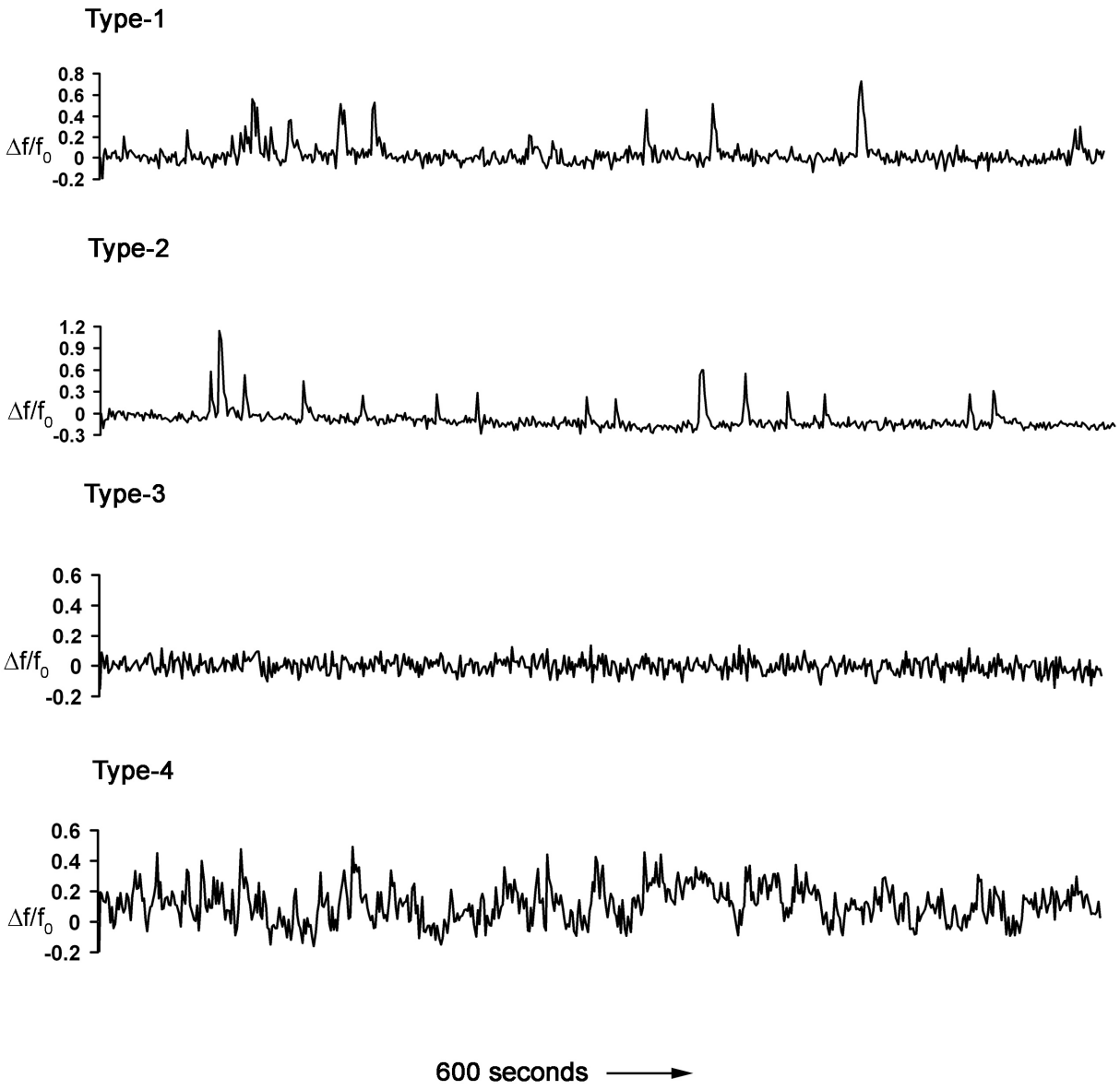

Figure 5.4 Modes of Ca^{2+} transients seen in 3DIV embryonic motoneurons.

5.4.I. Inhibitors of VGSC affect spontaneous Ca^{2+} elevation also in 100 nM TTX

In order to know if acute treatment of a potential sodium channel inhibitor is able to block calcium transients one of the highly firing cell of type 4 was analysed for acute treatment of 100 nM TTX. Motoneurons were loaded with the low-affinity calcium indicator dye Oregon Green BAPTA-1 (Kd =130 nm) for 15 minutes and cells were imaged in ASCF solution under continuous perfusion. In the Figure 5.5, a spontaneously active motoneuron is shown firing calcium transients for initial ten minutes. Addition of 100 nM TTX resulted in distinct blockade of excitability. When TTX is removed by perfusion with ACSF (washing period), spontaneous excitability was restored. This recovery of spontaneous calcium transients upon toxin removal could further be blocked and restored upon toxin removal (Figure 5.5). Interestingly, spontaneous Ca^{2+} transients were also seen in low-density cultures, under fast perfusion conditions (~20x ACSF exchange per min) in a slightly hyperpolarizing ACSF condition (extracellular 3mM K^{+}).

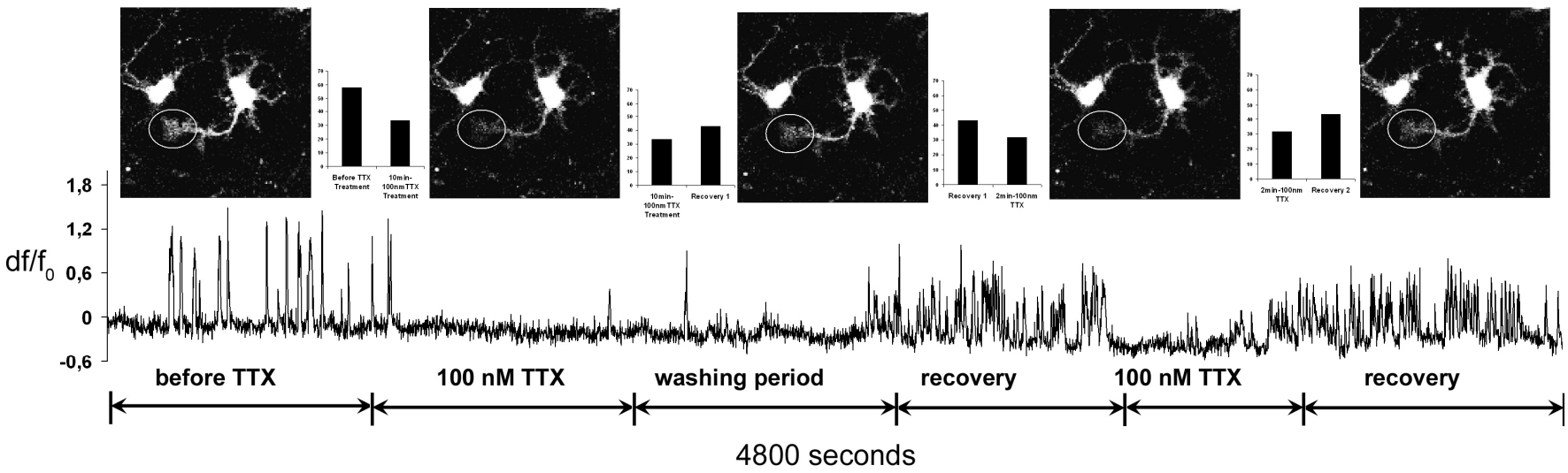

Figure 5.5 Excitable motoneurons are blocked by 100 nM TTX and are able to recover. High neural activity in a motoneuron was analysed for 10 minutes and 100 nM TTX was added at the end of 10th minute. Neural activity was blocked during the presence of TTX and was recovered after five minutes of washing period. Further addition of TTX for a short period of 2 minutes also blocked neural activity which recovered after washes.

5.4.II. Quantification of spontaneous excitability in cultured motoneurons

To standardize imaging conditions under various pharmacological conditions, the following strategy was chosen to quantify events of spontaneous Ca^{2+} elevation. Motoneurons that showed spontaneous calcium transients in a period of five minutes were then treated with corresponding concentrations of TTX or STX, for a period of five minutes to provide adequate time to for the toxin to block the permeabilization of sodium ions. At the end of five minutes cells were imaged for spontaneous calcium transients in the presence of TTX or STX for a period of five minutes. Next, cells were washed with ACSF to restore excitability and cells were reanalyzed after 10 minutes of toxin removal. The schematic representation to explain the quantification is shown in Figure 5.6

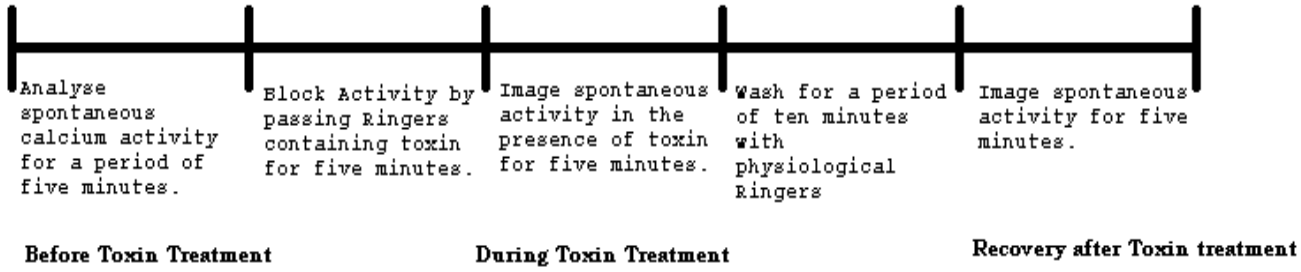

Figure 5.6 Schematic representation to quantify frequency of Ca^{2+} transients in response to pharmacological inhibition of sodium channels.

5.5. Spontaneous excitability is significantly reduced in cultured motoneurons in 100 nM TTX

Following the experimental flow chart (Figure.5.5), spontaneous Ca^{2+} transients were monitored in motoneurons (DIV3). VGSC were blocked by acute treatment of 100 nM TTX for a period of five minutes and further on motoneurons were allowed to recover. Frequency of calcium transients were counted before toxin treatment, in the presence of toxin and during recovery period and these results were quantified after background correction. Treatment of motoneurons with 100 nM TTX showed a significant reduction in neural activity at the cell body, distal axon and at the growth cone (Figure 5.7).

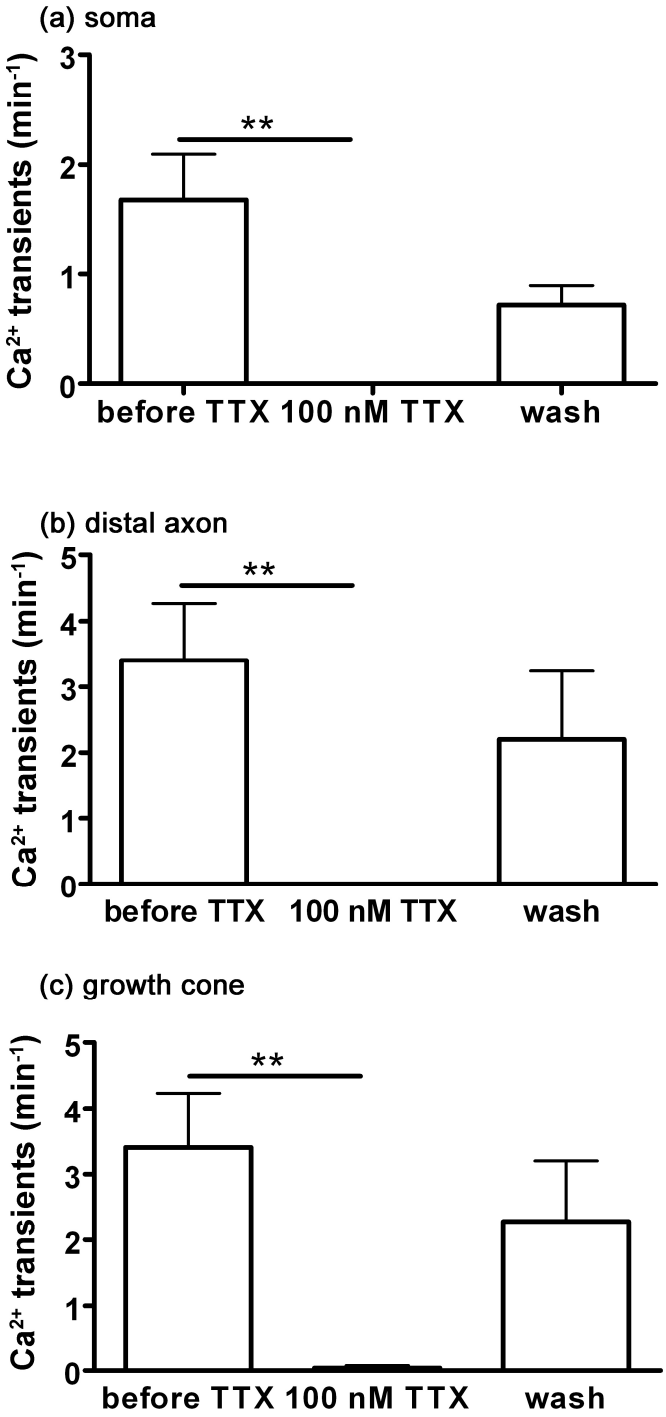

Figure 5.7 Spontaneous neural activity is blocked by 100 nM TTX. Quantification of spontaneous excitability in DIV3 cultured motoneurons in 100 nM TTX at (n=5) at the soma (a), distal axon (b) and growth cone (c) Results represent the mean ± SEM of pooled data from three independent experiments, n, number of motoneurons that were scored in total from control or toxin treated motoneurons. **, $P < 0.01$ tested by one-way ANOVA

5.6. Spontaneous excitability in cultured motoneurons is not affected by 10 nM TTX

To investigate the response of a lower dosage of TTX on neural excitability, a ten fold lower dosage of 10 nM TTX was tested on DIV3 embryonic motoneurons. The procedure followed was same as the pharmacological assay devised for quantification acute toxin treatments. On treatment with 10 nM TTX, neural excitability on DIV3 embryonic motoneurons did not show a significant reduction in the frequency of calcium transients, in comparison to the transients analyzed before toxin treatment. The figure 5.8 summarizes the quantification of frequency of calcium transients on 10 nM TTX treatments at the soma, distal axon and the growth cone of DIV3 embryonic motoneurons.

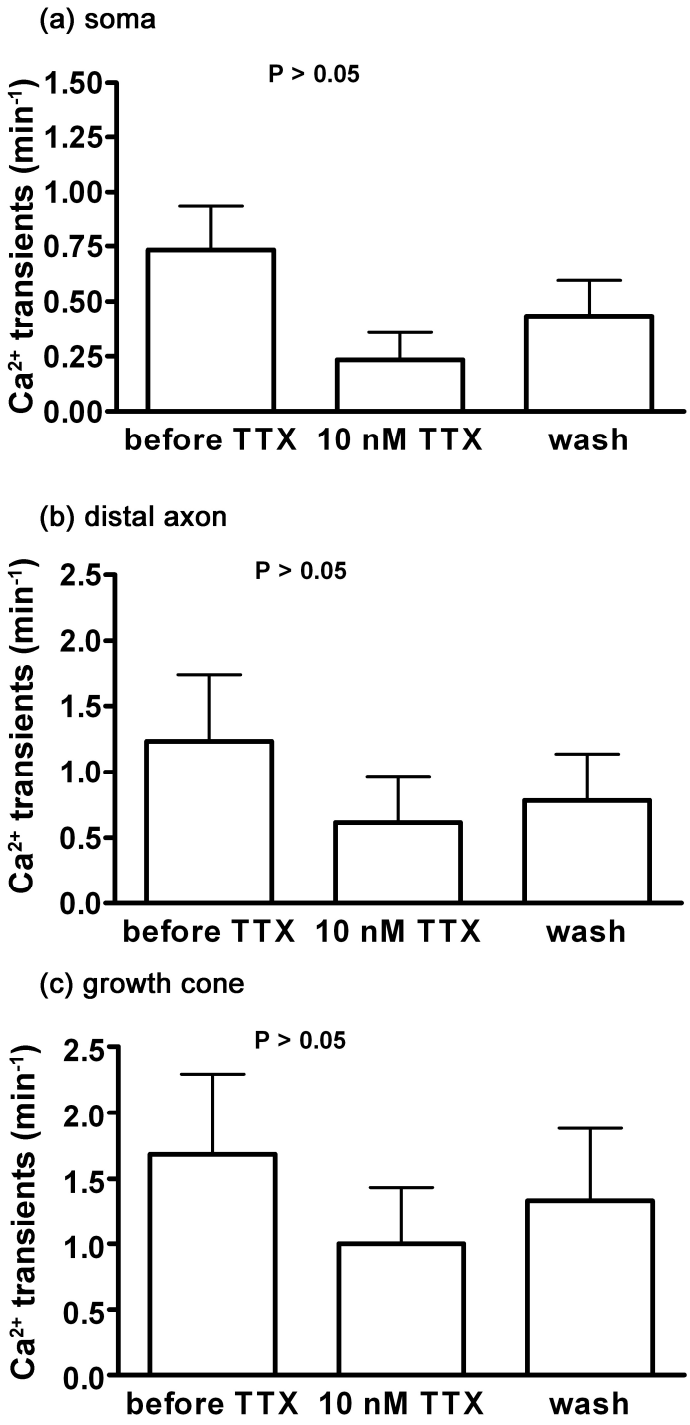

Figure 5.8 Spontaneous excitability is not blocked by 10 nM TTX. Quantification of spontaneous excitability in DIV3 cultured motoneurons in 10 nM STX (n=12). at the soma (a), distal axon (b) and growth cone (c) Results represent the mean ± SEM of pooled data from five independent experiments, n, number of motoneurons that were scored in total from control or toxin treated motoneurons. ***, $P < 0.001$ tested by one-way ANOVA.

5.7. Spontaneous excitability is reduced in cultured motoneurons in 10 nM STX.

It is known that in sodium channels with a higher TTX resistance, the channels $Na_V1.5$, Nav1.8, and $Na_V1.9$, carry a consensus protein motif in their pore-region, which indicates a pharmacological profile with a higher sensitivity to STX, in contrast to a certain resistance to TTX (Penzotti et al., 1998). Therefore we tested STX-sensitivity of spontaneous Ca^{2+} transients in motoneurons at DIV3. Pharmacological intrusion by 10 nM resulted in an almost complete blockade of neuronal excitability in growth cones (Fig. 7a). In contrast to TTX, 10 nM of STX was able to reduce spontaneous excitability in motoneurons (Fig. 5.9).

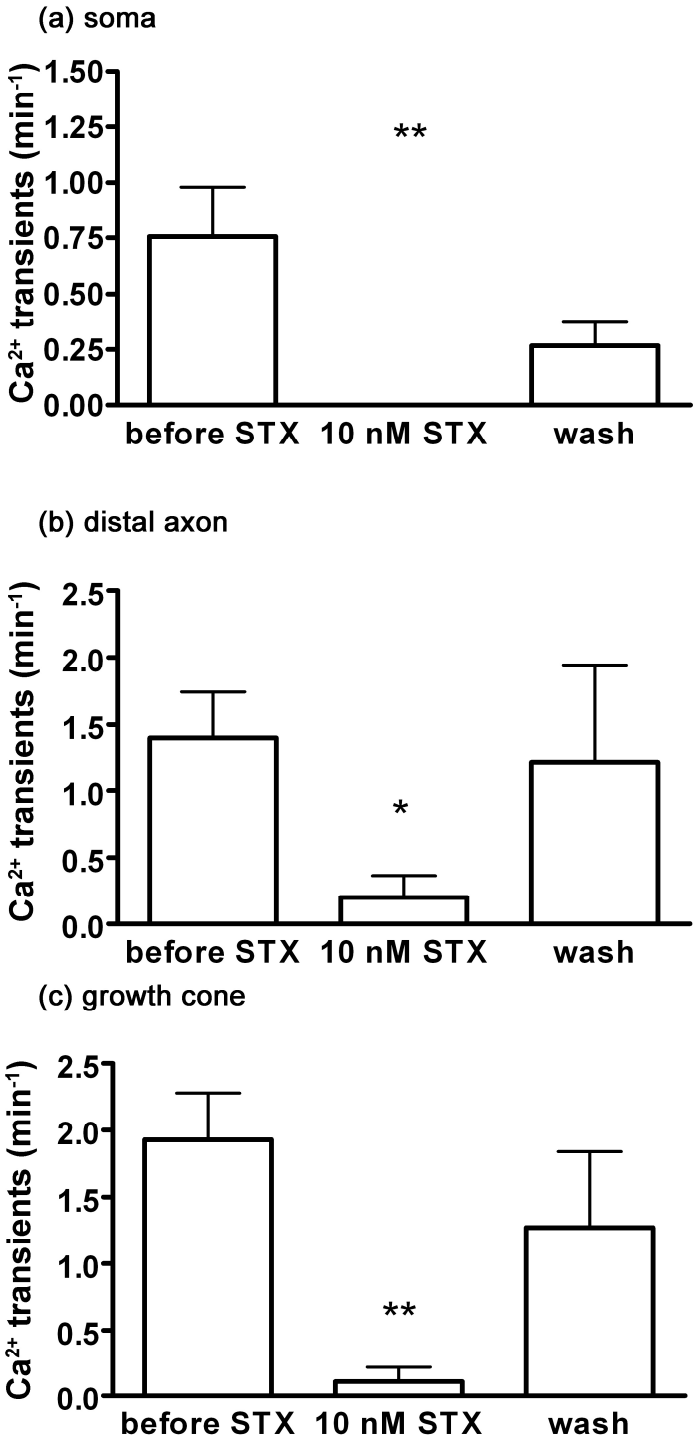

Figure 5.9 Spontaneous excitability is blocked by 10 nM STX (c). Quantification of spontaneous excitability in DIV3 cultured motoneurons in 10 nM STX (n=11). at the soma (a), distal axon (b) and growth cone (c) Results represent the mean ± SEM of pooled data from four independent experiments, n, number of motoneurons that were scored in total from control or toxin treated motoneurons. ***, $P < 0.001$ tested by one-way ANOVA.

5.8. Expression of $Na_V1.9$ in the lumbar spinal cord

The pharmacological inhibitions of VGSC on cultured motoneurons resulted in reduction in axon growth and neural activity. This was mainly achieved by lower doses of STX and not by high doses of TTX.. Previous studies in sensory neurons have shown that, the TTX resistant voltage-gated $Na_V1.9$ has very low activation threshold and is capable of eliciting spontaneous excitation at resting membrane potentials (Cummins et al., 1999; Herzog et al., 2001; Penzotti et al., 1998). $Na_V1.9$ has also been shown to be expressed in cultured hippocampal neurons and it has been responsible for high sensitivity to STX (10 nM) compared to TTX (50 nM). In this cell type, $Na_V1.9$ has been shown to be responsible for BDNF mediated excitation (Blum et al., 2002). Therefore I asked if $Na_V1.9$ is expressed in the spinal cord during late embryonic development. To test this, lumbar spinal cords were isolated at different stages of mouse development and RNA was isolated and reverse transcription PCR (RT-PCR) was performed. As a positive control, Nav1.6 and actin primers expression was monitored in parallel. As shown in Figure 5.10, expression of Nav1.9 could be seen starting from embryonic stage 16.

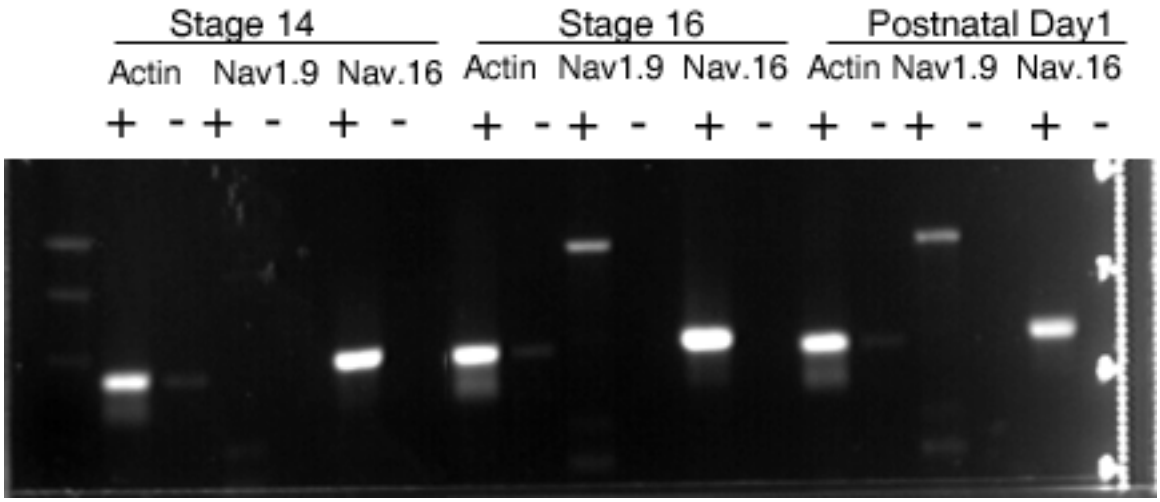

Figure 5.10 $Na_V1.9$ expression in mouse begins from embryonic stage 16

5.9. $Na_V1.9$ protein is concentrated in distinct axonal regions and growth cones of motoneurons

After confirming the presence of $Na_V1.9$ in the lumbar spinal cords at embryonic day (E) 16, peptide antibodies were generated against the 'C' terminal region of the mouse $Na_V1.9$ by Blum.R from our department. This antibody was tested for immunolocalization of $Na_V1.9$ in cultured motoneurons. At DIV3, when local spontaneous calcium transients are seen in axonal microdomains of axonal compartments and growth cones, anti- $Na_V1.9$ immunoreactivity was concentrated at the very same axonal subcompartments. In the somato-dendritic regions, $Na_V1.9$ was weakly labelled. It was also found that extracellular domains of TrkB and $Na_V1.9$ were found in the same subcompartments of axons and growth cones. The immunolabelling however were weakly co-localized, suggesting a close proximity of TrkB and $Na_V1.9$ (Figure 5.11). It is also shown further in this work that TrkB kinase deficient motoneurons show reduced axon growth and neural activity, independent of VGSC.

(a)

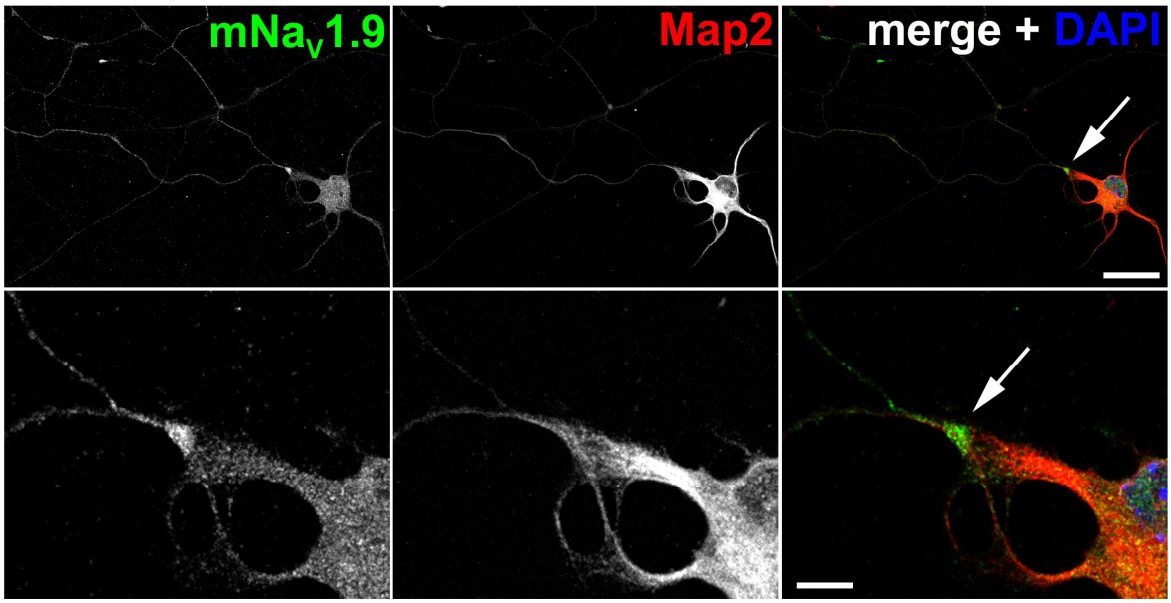

(b)

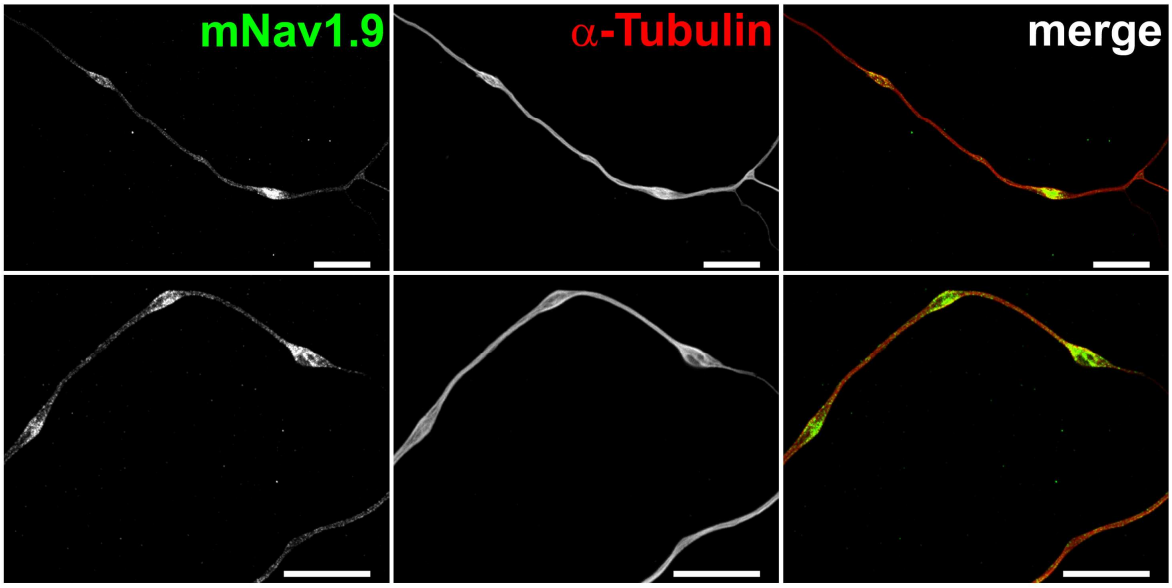

(c)

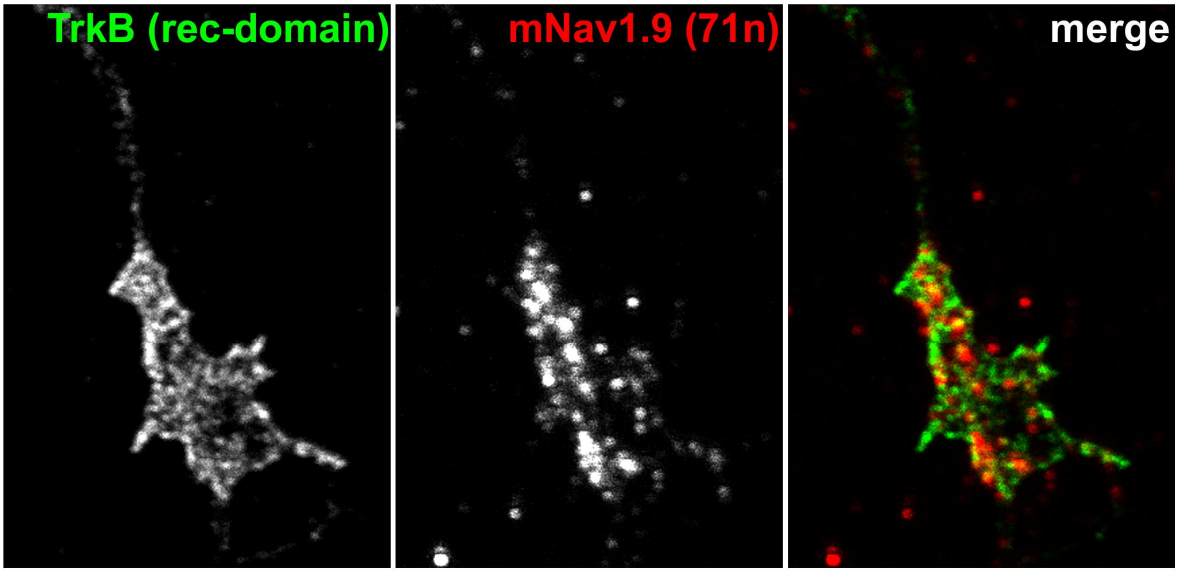

Figure 5.11 $Na_V1.9$ protein is concentrated in axonal compartments and growth cones of motoneurons.
(a) $Na_V1.9$ in green and dendritic marker Map2 in Red show a weaker staining for $Na_V1.9$ at the dendrites or the cell body.(b) $Na_V1.9$ (green) in axonal compartments, counterstained with α-tubulin (red). (c) $Na_V1.9$ (red) is seen in close proximity towards TrkB (green) at growth cones in motoneurons (DIV7). (Confocal images captured by Blum.R)

5.10. Knockdown of $Na_V1.9$ in cultured embryonic motoneurons reduces axon growth but not dendrite growth

The presence of $Na_V1.9$ expression in embryonic spinal cords prompted to investigate the importance of this gene in neurite growth. For this, the technique of RNA interference was utilized to knockdown $Na_V1.9$ using lentivirus mediated delivery. To generate the $Na_V1.9$ knockdown construct, short hairpin (sh) target sequences were chosen from the coding region of $Na_V1.9$ and this was cloned in lentiviral shRNA expression vectors under the promoter H1, as described in the methods section of this work. Two knockdown lentiviral constructs were generated one expressing GFP and the second one expressing tandem tomato as visualization markers. Lentiviruses were generated for each of the knockdown constructs and the corresponding scrambled constructs as per the three helper plasmid system as described in methods section. To introduce the knockdown shRNA and control /missense shRNA for $Na_V1.9$, freshly isolated motoneurons were transduced. For this, a 100µl volume of motoneurons suspensions containing 50000 cells were infected with high titre lentivirus-preparations expressing either sh $Na_V1.9$ or scrambled sh $Na_V1.9$. Then, infected motoneurons were cultured on laminin-111 coated cell culture dishes for a period of seven days in the presence of neurotrophic factors BDNF (10 ng/ml) and CNTF (10 ng/ml). At DIV7, motoneurons were stained with rabbit anti Tau and chicken anti GFP for cells infected with knockdown vector carrying GFP. Cells infected with lentiviral vectors carrying red florescence marker RFP were stained with β-tubulin and rabbit anti RFP [Figure 5.12 (a),(b)]. As evident from the figure, knockdown of $Na_V1.9$ resulted in shorter axons in comparison to controls (uninfected and missense), Figure 5.12 (a). The dendrite growth was unaffected,[Figure 5.12 (b)]. To rule out the toxicity of lentivirus on motoneurons, cell numbers were counted on the day of plating and then on the seventh day. As shown in Fig.5.12 (c), the percentage survival of motoneurons that were infected with lentiviruses

was not affected in the presence of survival neurotrophic factors. The quantification of axon growth on $Na_V1.9$ infection as shown in Figure 5.12 (d) & (e) reveals that $Na_V1.9$ knockdown regulates axon growth but not dendritic growth.

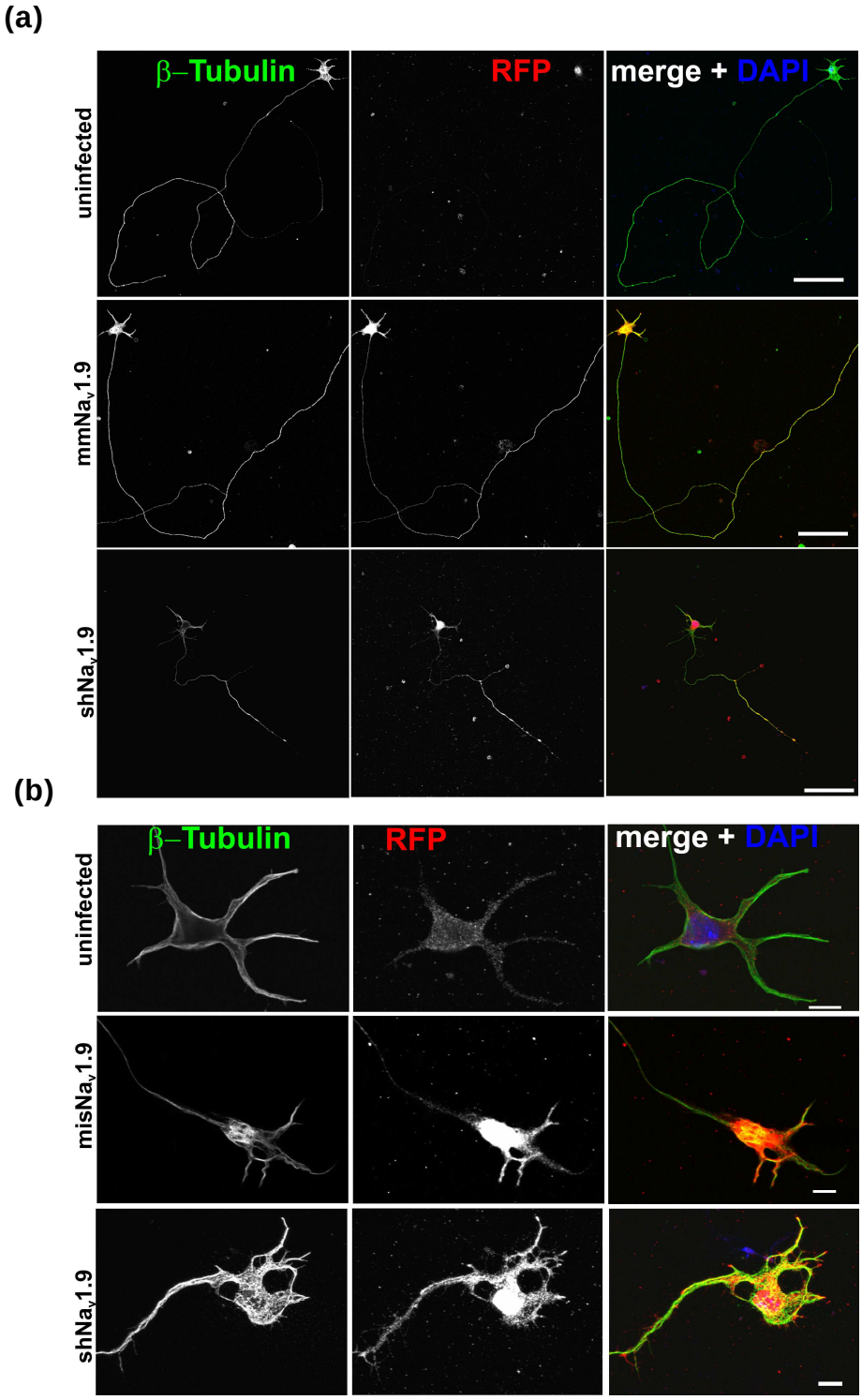

Figure 5.12 Axons are shorter in $Na_V1.9$ knockdown motoneurons (a), dendrites are not (b).
Immuno labelling of DIV7 motoneurons treated with sh $Na_V1.9$ and missense $Na_V1.9$ lentivirus. β-tubulin is labelled in green and infected motoneurons are labelled with red florescent protein. Scale bar: (a) 100µm (b) 10µm

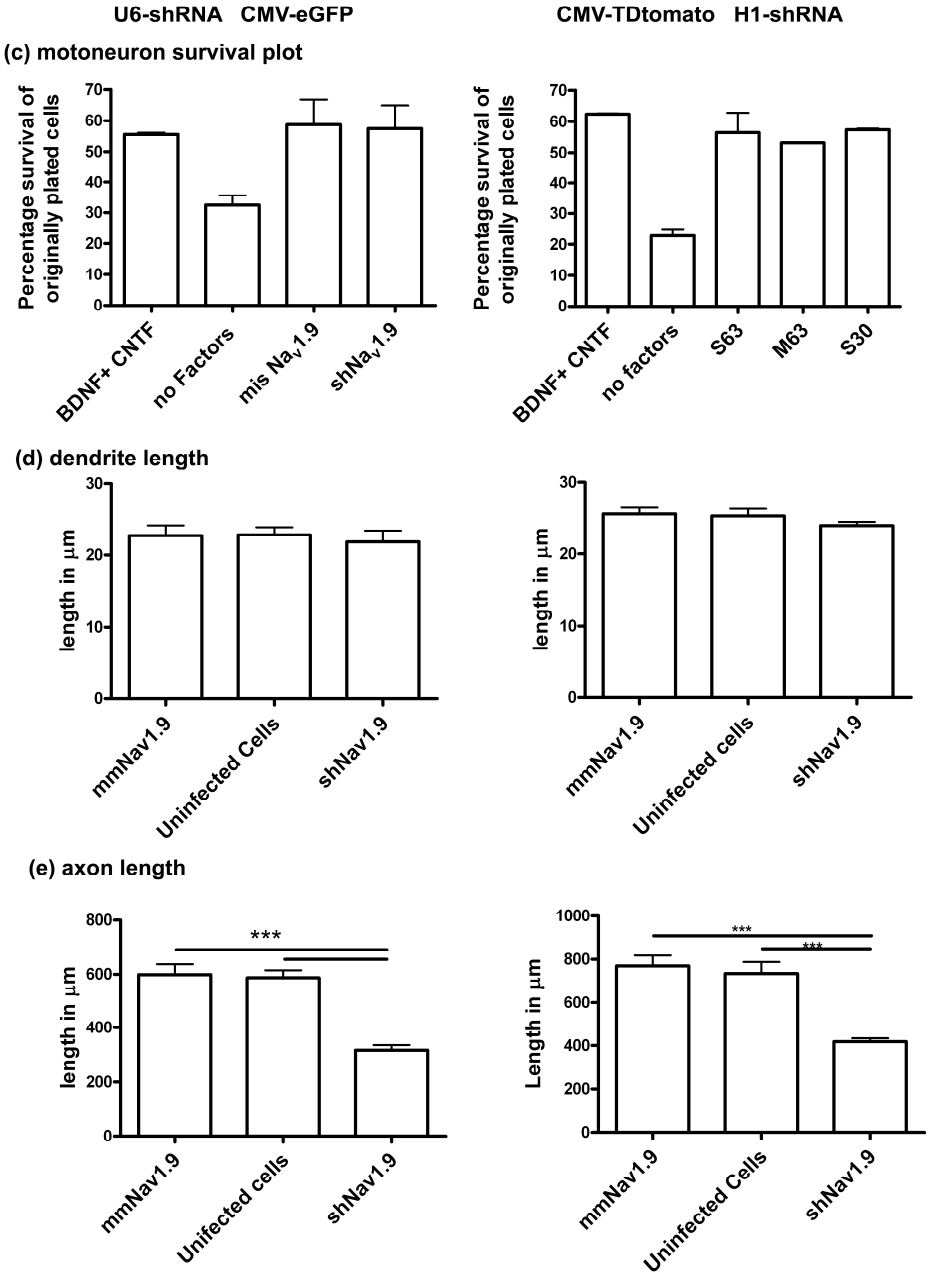

Figure 5.13 Knockdown of $Na_V1.9$ in cultured motoneurons reduces axon length but dendrites are unaffected.
Survival (c) was quantified from three independent survival tests.(d) dendrite length and (e) axon length was measured from lentivirus infected motoneurons containing U6 shRNA with CMV eGFP vector, [uninfected (n= 134), mis $Na_V1.9$ (n= 65), sh $Na_V1.9$ (n=65)] or CMV TDtomato h1-shRNA [uninfected (n= 67), mis $Na_V1.9$ (n= 108), sh $Na_V1.9$ (n=105)]. Results represent the mean ± SEM of pooled data from three independent experiments, n= number of motoneurons that were scored in total from control or lentivirus treated motoneurons.***,P<0.0001 tested by one-way ANOVA.

5.11. Neurite growth and neural excitability is reduced in cultured $Na_V1.9^{-/-}$ motoneurons

To further validate the $Na_V1.9$ knockdown observations in cultured motoneurons by lentivirus mediated shRNA, the neurite growth phenotype in $Na_V1.9$ deficient mouse was also analyzed. The $Na_V1.9$ deficient mice were provided John Wood, and Mohammed A. Nassar (Wolfson Institute of Biomedical Research, University College London,UK) In the $Na_V1.9^{-/-}$ mice the exons 4 and 5 from the gene *SCN11A* was replaced by a neomycin resistance cassette that removes that S4 voltage sensing region of $Na_V1.9$. These $Na_V1.9^{-/-}$ were homozygous viable and were shown to be required for G-protein pathway-regulated TTX resistant sodium current in sensory neurons (Ostman et al., 2008)

5.11.I. $Na_V1.9$ is not required for motoneuron survival.

Pharmacological inhibition of VGSC did not affect motoneuron survival. In order to re-confirm this, embryonic motoneurons from lumbar spinal cords from embryonic day (E14) from $Na_V1.9^{-/-}$ mice were cultured as described for wildtype motoneurons. The motoneurons were cultured for a period of seven days in congruence with previous experiments in this work. A percentage survival of motoneurons was calculated from two independent cultures at the end of day seven. It was found that survival of $Na_V1.9^{-/-}$ motoneurons were not affected when compared to those grown in the absence of survival neurotrophic factors BDNF and CNTF (10 ng/ml). This shows that absence of $Na_V1.9^{-/-}$ does not play a role in motoneuron survival (Figure 5.14).

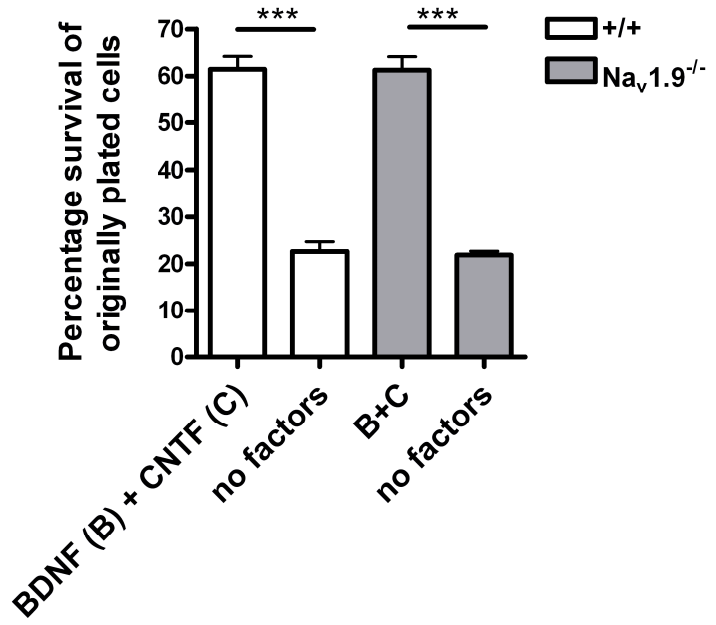

Figure 5.14 Absence of Nav1.9 does not affect survival of cultured motoneurons. Motoneurons were plated at a density of 5000 cells/well, and survival was determined after 7 d in culture. Survival rates of motoneurons were performed on wild type and $Na_V1.9^{-/-}$ motoneurons Results represent the mean ± SEM of pooled data from two independent experiments. **, P<0.0001 tested by *t* test.

5.11.II. $Na_V1.9$ is absent in axonal regions of $Na_V1.9^{-/-}$ mice

Immunocytological experiments confirmed the presence of for $Na_V1.9$ at the growth cones and axonal compartments of cultured embryonic motoneurons. To confirm this finding we analysed cultured embryonic motoneurons from $Na_V1.9^{-/-}$ mice. At the end of seven days motoneurons were fixed and immunolabelled for anti $Na_V1.9$-(71n) and counter stained with anti α-tubulin. As shown in the Figure 5.14, $Na_V1.9$ deficient motoneurons show distinct absence of anti-$Na_V1.9$ (71n) signals in the growth cones and axon compartments in comparison to wild type motoneurons.

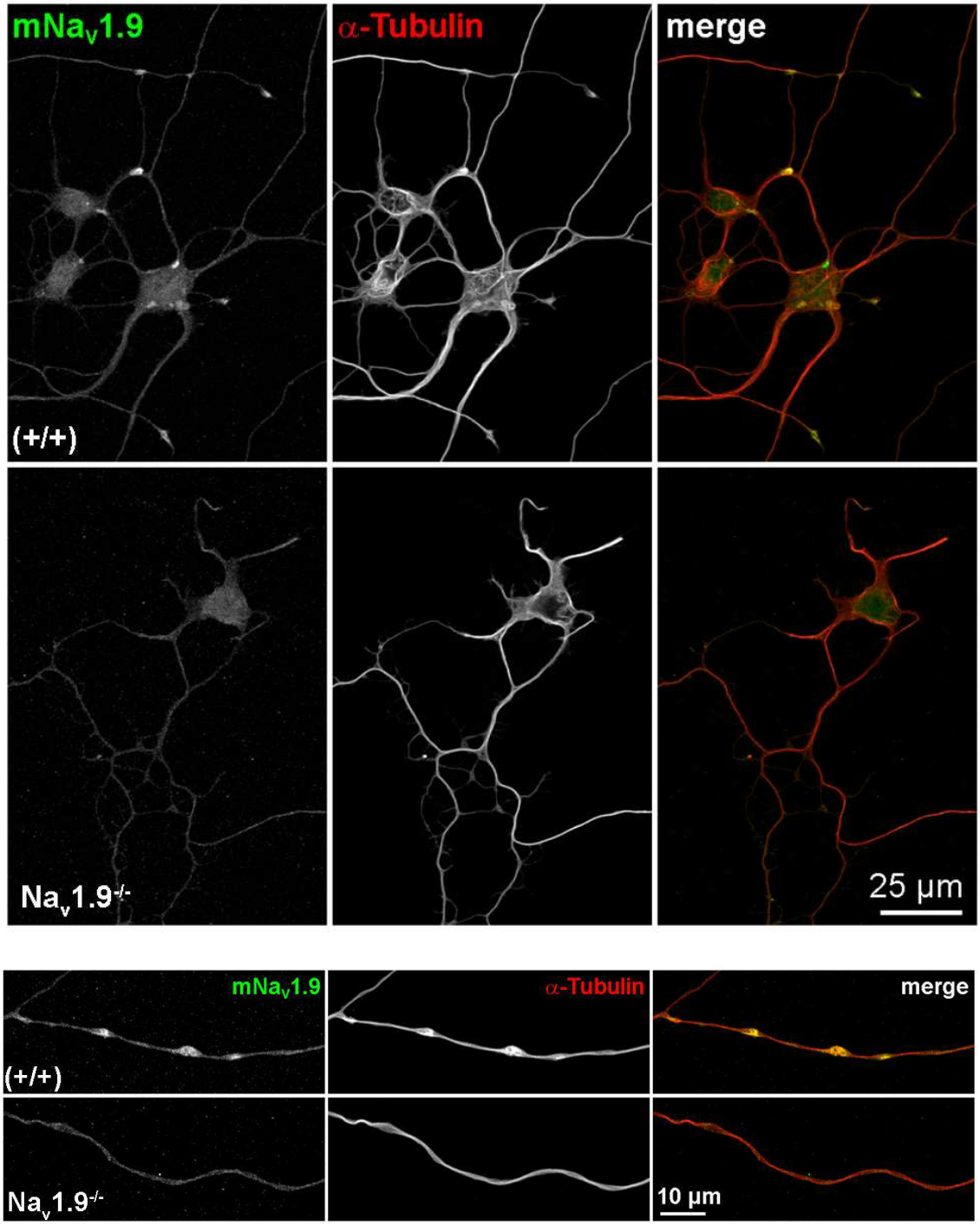

Figure 5.15 Na$_V$1.9 protein is highly reduced in Na$_V$1.9 deficient mice. Immunolabelling of Na$_V$1.9 is reduced in the axonal compartments in comparison to the wild type motoneurons (DIV7). α-tubulin used as a control marker (Confocal images captured by Blum.R)

5.11.III. $Na_V1.9^{-/-}$ embryonic motoneurons show reduced axon length in cultured motoneurons, dendrites are unaffected.

The *in vitro* knockdown of $Na_v1.9$ by lentiviral shRNA expression resulted in a significant reduction of axon length in cultured motoneurons. It was therefore imperative to analyse the embryonic motoneurons from $Nav1.9^{-/-}$ mice. Embryonic motoneurons were cultured from $Na_V1.9^{-/-}$ mice and motoneurons were fixed at DIV7 and immunolabelled with anti-Tau or anti β-tubulin to perform axon length measurements. Indeed, the axon length of cultured embryonic $Na_V1.9^{-/-}$ motoneurons was reduced in comparison to motoneurons from wild type animals (Figure 5.16). The dendrite length in both wild type and $Na_v1.9$ motoneurons remained unchanged (Figure 5.16). This experiment confirmed that $Na_v1.9$ plays an important role in axon elongation in cultured motoneurons.

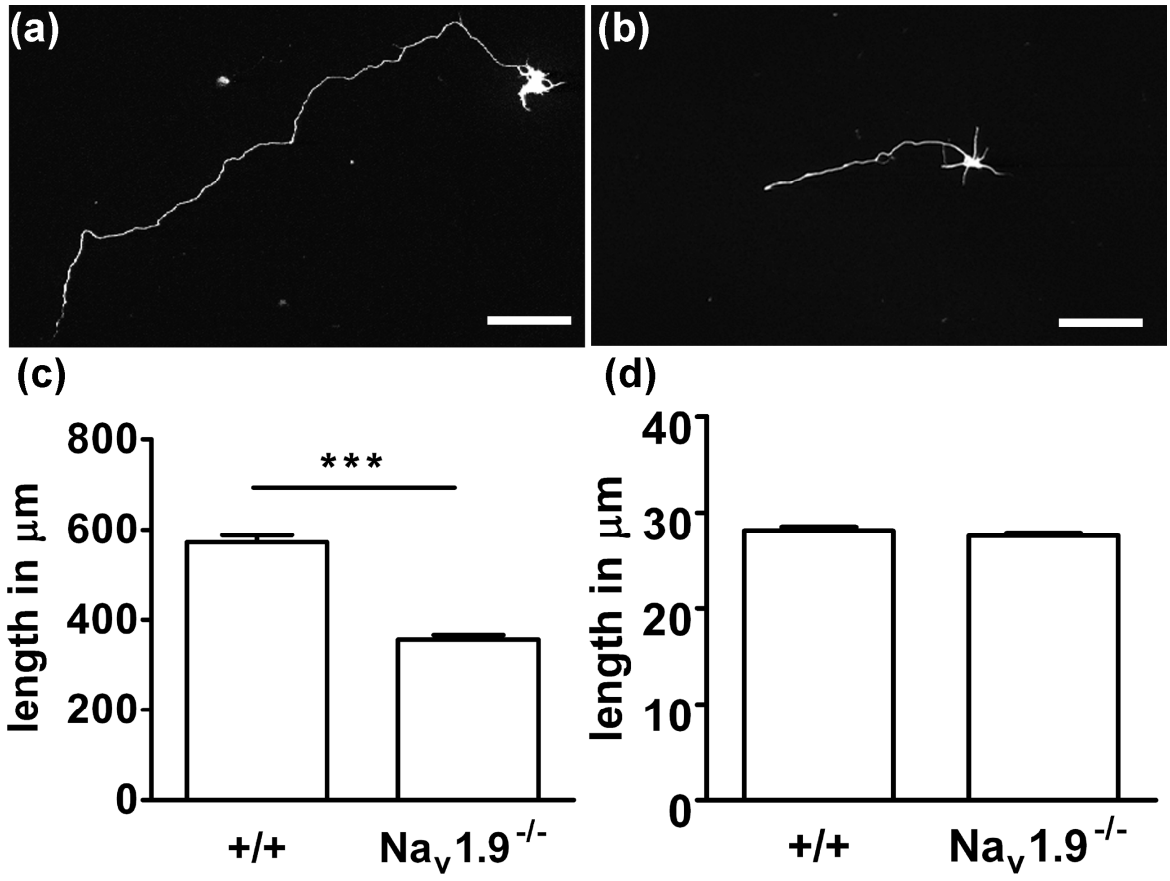

Figure 5.16 $Na_V1.9^{-/-}$ mice show reduced axon length but dendrite length remains unchanged. (a) Wildtype and (b) $Na_V1.9^{-/-}$ motoneuron stained with α-Tau.(c) Quantified axon length (n=447 and (d) dendrite length(n=286). Results represent the mean ± SEM of pooled data from three independent experiments. n, number of motoneurons that were scored in total from control or lentivirus treated motoneurons.***,P<0.0001 tested by t test. Scale bar-100µm

5.11.IV. $Na_V1.9$ regulates neural activity in embryonic motoneurons

In order to check the role of $Na_V1.9$ in spontaneous neural activity, frequency of Ca^{2+} transients were analyzed in motoneurons from wild type and $Na_V1.9^{-/-}$ animals at DIV3 as described above As shown in figure 5.17, the frequency of calcium transients is significantly reduced at the growth cone, distal axon and the cell body of cultured motoneurons, in comparison to wild type motoneurons. This confirms that $Na_V1.9^{-/-}$ plays an important role in the regulation of neural activity in cultured motoneurons

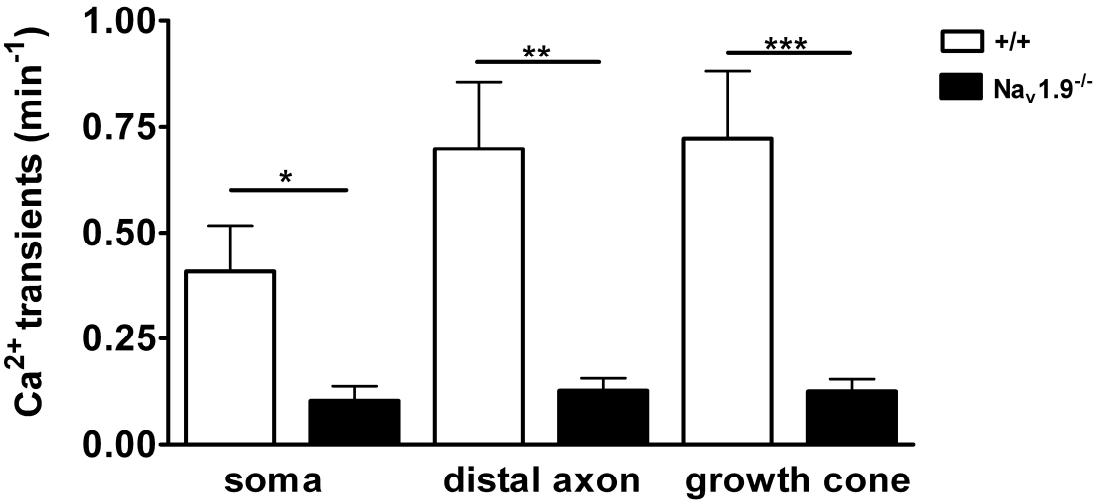

Figure 5.17 $Na_V1.9^{-/-}$ mice show reduced neural activity at the growth cone, distal axon and the cell body in cultured motoneurons. Results represent the mean ± SEM of pooled data from four independent experiments. +/+, n=80 and $Na_v1.9^{-/-}$ n= 138 , number of motoneurons that were scored in total from control or $Na_V1.9^{-/-}$ motoneurons.***,P<0.0001 **,P<0.001 and *,P<0.01, as tested by t tests.

5.12. Excitability and neurite growth is reduced in TrkB$^{TK-/-}$ motoneurons

It had been described that the open probability of the sodium channel Nav1.9 is increased by activation of TrkB receptor tyrosine kinesis. Therefore we asked if the absence of TrkB function influences neurite outgrowth of motoneurons and whether this growth effect is dependent on VGSC. Neurite growth and cellular excitability was investigated in motoneurons isolated from TrkB knockout mice in which the kinase region of the receptor was specifically affected. Here, TrkB motoneurons were cultivated for a period of five days and neuronal excitability was checked in TrkB knockout cells and wild type littermates as a control. As shown in Figure 5.18, TrkB knockout motoneurons showed a reduced axon length and a reduced frequency of spontaneous Ca^{2+} transients in comparison to their wild-type littermates. Interestingly treatment of TrkB$^{TK-/-}$ with 100 nM STX does not further affect the length of TrkB$^{TK-/-}$ motoneurons.

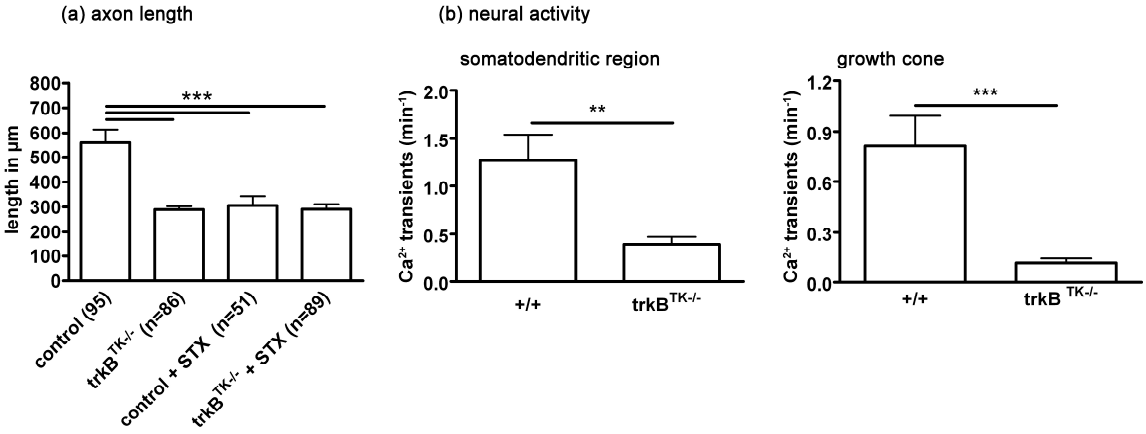

Figure 5.18 Neurite growth and excitability is reduced in TrkB knockout motoneurons.
(a) axon length (DIV7), (b) neural activity (DIV5), (+/+,n=15, trkB$^{TK-/-}$, n=40) .Results represent the mean ± SEM of pooled data from three independent experiments. n, number of motoneurons that were measured for length in total from control or trkB $^{TK-/-}$ motoneurons.***,P<0.0001 tested by one-way ANOVA for axon length (a) and t tests for neural activity (b).

6. Discussion

Embryonic motoneurons exhibit spontaneous neural activity when they send out their axons to reach out towards skeletal muscles. In the motoneurons of the developing rodents and chick embryo, this spontaneous activity has been shown consisting of rhythmic bursts of electrical activity which is necessary for axon path finding, synaptic maturation and number of important developmental processes (Branchereau et al., 2000; Metzger et al., 2000; Milner and Landmesser, 1999; Nishimaru et al., 1996; Ren and Greer, 2003) . Earlier studies in very young lumbar motoneurons have demonstrated that first step in triggering activity-dependent developmental programs is the regulation of Ca^{2+} influx (Metzger et al., 2000; Moody and Bosma, 2005). The work presented here is based on investigation of the role of TTX resistant VGSC in activity dependent axon growth in embryonic cultured motoneurons. With the help of pharmacological inhibition of VGSCs by neurotoxins, their role in motor axon growth was established. Evidences from dosage based blockade of sodium channels by two different neurotoxins STX and TTX and RT-PCR experiments, resulted in the prediction of $Na_v1.9$ as one of the TTX-insensitive isoform of VGSCs. Further shRNA mediated knockdown and analysis of $Na_V1.9$ knockout mice, confirmed a novel involvement of $Na_v1.9$ in axon elongation and regulation spontaneous neural activity in cultured embryonic motoneurons. The important implications of the findings of this work are the main focus of this discussion.

6.1. Activity dependent axon growth is regulated by VGSC.

Axon path-finding towards precise targets is a crucial part of embryonic development. Earlier studies have shown that spinal motor axons reach out towards their muscle targets via activity independent mechanisms (Huang et al., 2003; Lewis and Eisen, 2003; Schneider and Granato, 2003), thereby following a consensus that electric activity occurs after synapse formation at the target areas. On the other hand further studies have highlighted that activity dependent growth of axons occur when axons elongate (Borodinsky et al., 2004; Hanson and Landmesser, 2004) and also that these young differentiating neurons form synapses at intermediate points before reaching their muscle targets (Lefebvre et al., 2004). The activity dependent forms of cellular events like axon growth are regulated by intrinsic forms of spontaneous neural activity that are evident in excitable cells such as spinal motoneurons (Ming et al., 2001; O'Donovan et al., 1998; Spitzer et al., 1995). VGSC have been known to play a key role in regulating neural activity (Catterall, 1984; Chen et al., 2004). In accordance to these findings, when neural activity was pharmacologically blocked by sodium channel inhibitors STX and TTX resulted in significant reduction in frequency of Ca^{2+} transients at the cell body, distal axons and the growth cones. It was also shown in this work that lower dosages of STX are sufficient to block neural activity in comparison to TTX. These results provided important hint to the role of TTX insensitive sodium channels that could play a crucial role in regulating neural activity. Previous studies have shown that spontaneous Ca^{2+} transients in cultured embryonic motoneurons are important for axon elongation and neural activity (Jablonka et al., 2007). It was also found in this study that lower doses of STX are sufficient to significantly reduce motor axon growth in embryonic cultured motoneurons in comparison to TTX. These results therefore highlight the role of TTX insensitive VGSC to regulate neurite growth and spontaneous activity in embryonic cultured motoneurons.

6.2. $Na_v1.9$ regulates Ca^{2+} transients and axon elongation in cultured motoneurons

Several lines of evidence pointed to $Na_V1.9$ as best candidate among the TTX insensitive sodium channels that regulates axon growth and neural activity. First, $Na_V1.9$ has a low activation threshold which is close to the resting membrane potential. Second, the channel carries a specific motif in its channel pore domain, where the sodium channel blockers TTX and STX bind. This motif is an amino acid substitution of phenylalanine (F) or tyrosine (Y) to a cysteine (C) or a serine (S) residue at the domain I (Catterall, 2000; Penzotti et al., 1998; Sivilotti et al., 1997) This exchange reduces the binding affinity of TTX in this region, while STX binding affinity is less affected. Indeed the TTX insensitive VGSC $Na_V1.9$ was detected in the embryonic spinal cords from stage sixteen of the mouse development. This channel is known to be one of the predominantly expressed gene in the peripheral nervous system (Benn et al., 2001; Cummins et al., 1999; Dib-Hajj et al., 2002; Ostman et al., 2008; Rush and Waxman, 2004). Earlier the presence of $Na_v1.9$ in the central nervous system was confirmed by electrophysiological studies on fast excitatory currents in hippocampal neurons by the application of neurotrophin BDNF via its receptor TrkB (Blum et al., 2002; Lang et al., 2007).

The $Na_V1.9$ channel has a unique property among the nine VGSC isoforms, in having a reduced threshold of channel activation of -70mV, wherein the channel remains in an opened state at the near resting membrane potential (Cummins et al., 1999; Herzog et al., 2001; Ostman et al., 2008; Rugiero et al., 2003). Hence it would be less likely that any of the other eight members of the sodium channel family could complement the absence of $Na_V1.9$. This property could also prove as a drawback for $Na_V1.9$ in motoneurons due to its reduced expression as revealed in the immunolabelling experiments and thereby increasing the probability of remaining in a near opened state. This would also imply that

spontaneous neural activity that is read out by measuring frequency of Ca^{2+} transients in mouse embryonic cultured motoneurons, are most likely regulated by $Na_V1.9$.

Although embryonic cultured motoneurons from the $Na_V1.9$ deficient mice show reduced axon growth, the $Na_V1.9$ deficient mice do not show any severe phenotype related to motoneuron degeneration (Leo et al., 2010). These mice are devoid of any functional defects due to shorter axons found *in vitro*. This could possibly imply that the spinal motoneurons in $Na_V1.9$ deficient mice are able to reach their skeletal muscles. Firstly this effect could be explained by existence so far unknown compensatory mechanisms. At the same time when compared to other mouse models like SMA where the levels of smn proteins are reduced, embryonic motoneurons cultured from smn deficient animals show reduced neural activity, axon elongation and defective Ca^{2+} clustering at the growth cones (Jablonka et al., 2007; Rossoll et al., 2003). In spite of reduction in axon growth observed in cultured motoneurons, the loss of motoneuron cell bodies in the smn deficient mice, does not exceed more than 20%, implying that most of these motoneurons develop normally during embryonic motoneuron differentiation and they are thus able to reach their skeletal muscle targets (Monani et al., 2000).

6.3. Motoneuron survival before synapse formation does not need sodium channel activity.

The pharmacological experiments in this study show that conditions that inhibit spontaneous Ca^{2+} influx via the blockade of VGSC do not affect motoneurons survival. This also rules out the toxic effects of the inhibitors of sodium channels. Previous studies have shown that pharmacological inhibition of VGSC, of developing retinal ganglion cells reduces their survival (Kaiser and Lipton, 1990; Lipton, 1986). While the Lipton et al, study mainly focused on activity dependent survival of RGCs, and predicted the requirement of a tropical survival factors for

normal survival of RGCs, the motoneuron culture system utilized here has been constantly undertaken in the presence of survival neurotrophic factors namely, BDNF and CNTF. Thus it rules out the selective survival of sub-population of motoneurons that could show reduction in axon growth. The finding that embryonic cultured motoneurons from $Na_V1.9^{-/-}$ did not affect motoneuron survival, excludes any inference of $Na_V1.9$'s role in activity dependent survival in spinal motoneurons.

6.4. $Na_V1.9$ behaves as an upstream switch that triggers spontaneous Ca^{2+} influx.

The neurotrophin BDNF has been shown in previous studies as a modulator of activity dependent synaptic plasticity and maturation (Kuczewski et al., 2009; Thoenen, 2000). In this context, studies have also shown that excitatory actions of BDNF/TrkB signalling on mature hippocampal neurons elicit TTX resistant sodium channels (Kafitz et al., 1999) and this activation is upstream of activation of voltage-dependent calcium channels (Kovalchuk et al., 2002). The study emphasized the role of BDNF in rapid Ca^{2+} influx in dendritic spines of mature hippocampal neurons thereby indicating that such a mechanism is upstream of voltage-dependent calcium channels. Further the group of Blum et al provided strong evidences by RT-PCR screening, antisense expression and heterologous reconstitution in HEK293 cells, that $Na_V1.9$ is responsible for excitatory actions of BDNF through TrkB kinase activation (Blum et al., 2002).

In the case of embryonic cultured motoneurons, what modulates $Na_V1.9$ to regulate activity dependent axon growth is not clearly known. The analysis of $TrkB^{TK-/-}$ deficient motoneurons on treatment with STX showed no further reduction in motor axon growth, thereby suggesting neurotrophin independent channel activation. Moreover, the embryonic cultured motoneurons were constantly in the presence of BDNF as a

motoneuron survival factor, at concentrations of 10ng/ml. At these concentrations, the possibility of membrane bound TrkB is saturated so as to prohibit the binding of BDNF that might be spontaneously released from the cultured motoneurons. In this scenario, it can be speculated that the opening of $Na_V1.9$ could be mediated via transactivation of TrkB receptors that are not seen at the cell membrane.

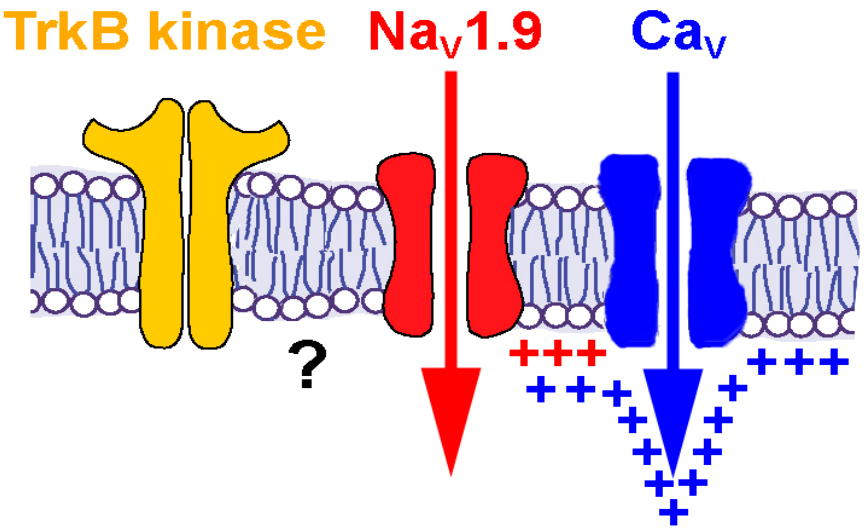

Figure 6.1 $Na_v1.9$ is an upstream switch to trigger spontaneous Ca^{2+} influx (Figure designed by R.Blum).

6.5. $Na_V1.9$: A therapeutic target for axonal regeneration

Mouse models of motoneuron diseases have been useful in understanding the phathophysiology and mechanisms involved in motoneuron degeneration. The pathways involved in motoneuron differentiation and axon elongation give valuable insights to develop therapeutic strategies to counteract motoneuron diseases like spinal muscular atrophy (SMA), amyotrophic lateral sclerosis (ALS), progressive motor neuronopathy, (pmn) (Schmalbruch et al., 1991), or neuromuscular degeneration (nmd) (Cox et al., 1998). So far most of the studies related to voltage-gated $Na_v1.9$ has been known focused on its pain-related nociceptive signalling due its predominant expression in the peripheral nervous system (Baker et al., 2003; Dib-Hajj et al., 2002; Krafte and Bannon, 2008; Leo et al., 2010; Wood et al., 2004a; Wood et al., 2004b) It has been shown for the first time in this study, that $Na_v1.9$ is expressed in embryonic spinal motoneurons. The findings presented here highlight the role of $Na_v1.9$ in activity dependent axon elongation in embryonic cultured motoneurons. Studies on primary sensory neurons have revealed the activation of $Na_V1.9$ via G-protein signalling pathways (Ostman et al., 2008; Rush and Waxman, 2004). The fact that $Na_V1.9$ has very low activation threshold gives rise to the probability of keeping the channel in opened state by extrinsic cues. $Na_V1.9$ could thus prove to be a potential therapeutic target for axonal regeneration in mouse models of motoneuron disease.

7. References

Baker, M.D., Chandra, S.Y., Ding, Y., Waxman, S.G., and Wood, J.N. (2003). GTP-induced tetrodotoxin-resistant Na+ current regulates excitability in mouse and rat small diameter sensory neurones. J Physiol *548*, 373-382.

Benn, S.C., Costigan, M., Tate, S., Fitzgerald, M., and Woolf, C.J. (2001). Developmental expression of the TTX-resistant voltage-gated sodium channels Nav1.8 (SNS) and Nav1.9 (SNS2) in primary sensory neurons. J Neurosci *21*, 6077-6085.

Birnboim, H.C., and Doly, J. (1979). A rapid alkaline extraction procedure for screening recombinant plasmid DNA. Nucleic Acids Res *7*, 1513-1523.

Bixby, J.L., and Spitzer, N.C. (1984). Early differentiation of vertebrate spinal neurons in the absence of voltage-dependent Ca2+ and Na+ influx. Dev Biol *106*, 89-96.

Blum, R., Kafitz, K.W., and Konnerth, A. (2002). Neurotrophin-evoked depolarization requires the sodium channel Na(V)1.9. Nature *419*, 687-693.

Bootman, M.D., Lipp, P., and Berridge, M.J. (2001). The organisation and functions of local Ca(2+) signals. J Cell Sci *114*, 2213-2222.

Borodinsky, L.N., Root, C.M., Cronin, J.A., Sann, S.B., Gu, X., and Spitzer, N.C. (2004). Activity-dependent homeostatic specification of transmitter expression in embryonic neurons. Nature *429*, 523-530.

Branchereau, P., Morin, D., Bonnot, A., Ballion, B., Chapron, J., and Viala, D. (2000). Development of lumbar rhythmic networks: from embryonic to neonate locomotor-like patterns in the mouse. Brain Res Bull *53*, 711-718.

Brummelkamp, T.R., Bernards, R., and Agami, R. (2002). A system for stable expression of short interfering RNAs in mammalian cells. Science *296*, 550-553.

Burns, J.C., Friedmann, T., Driever, W., Burrascano, M., and Yee, J.K. (1993). Vesicular stomatitis virus G glycoprotein pseudotyped retroviral vectors: concentration to very high titer and efficient gene transfer into mammalian and nonmammalian cells. Proc Natl Acad Sci U S A *90*, 8033-8037.

Catterall, W.A. (1984). The molecular basis of neuronal excitability. Science *223*, 653-661.

Catterall, W.A. (2000). From ionic currents to molecular mechanisms: the structure and function of voltage-gated sodium channels. Neuron *26*, 13-25.

Chen, C., Westenbroek, R.E., Xu, X., Edwards, C.A., Sorenson, D.R., Chen, Y., McEwen, D.P., O'Malley, H.A., Bharucha, V., Meadows, L.S., *et al.* (2004). Mice lacking sodium channel beta1 subunits display defects in neuronal excitability, sodium channel expression, and nodal architecture. J Neurosci *24*, 4030-4042.

Chou, S.M., and Norris, F.H. (1993). Amyotrophic lateral sclerosis: lower motor neuron disease spreading to upper motor neurons. Muscle Nerve *16*, 864-869.

Cox, G.A., Mahaffey, C.L., and Frankel, W.N. (1998). Identification of the mouse neuromuscular degeneration gene and mapping of a second site suppressor allele. Neuron *21*, 1327-1337.

Cui, Q. (2006). Actions of neurotrophic factors and their signalling pathways in neuronal survival and axonal regeneration. Mol Neurobiol *33*, 155-179.

Cummins, T.R., Dib-Hajj, S.D., Black, J.A., Akopian, A.N., Wood, J.N., and Waxman, S.G. (1999). A novel persistent tetrodotoxin-resistant sodium current in SNS-null and wild-type small primary sensory neurons. J Neurosci *19*, RC43.

deLapeyriere, O., and Henderson, C.E. (1997). Motoneuron differentiation, survival and synaptogenesis. Curr Opin Genet Dev *7*, 642-650.

Desarmenien, M.G., and Spitzer, N.C. (1991). Role of calcium and protein kinase C in development of the delayed rectifier potassium current in Xenopus spinal neurons. Neuron *7*, 797-805.

Dib-Hajj, S., Black, J.A., Cummins, T.R., and Waxman, S.G. (2002). NaN/Nav1.9: a sodium channel with unique properties. Trends Neurosci *25*, 253-259.

Dull, T., Zufferey, R., Kelly, M., Mandel, R.J., Nguyen, M., Trono, D., and Naldini, L. (1998). A third-generation lentivirus vector with a conditional packaging system. J Virol *72*, 8463-8471.

Feller, M.B. (1999). Spontaneous correlated activity in developing neural circuits. Neuron *22*, 653-656.

Gomez, T.M., and Zheng, J.Q. (2006). The molecular basis for calcium-dependent axon pathfinding. Nat Rev Neurosci *7*, 115-125.

Greensmith, L., and Vrbova, G. (1997). Disturbances of neuromuscular interaction may contribute to muscle weakness in spinal muscular atrophy. Neuromuscular Disorders *7*, 369-372.

Grumbles, R.M., Sesodia, S., Wood, P.M., and Thomas, C.K. (2009). Neurotrophic factors improve motoneuron survival and function of muscle reinnervated by embryonic neurons. J Neuropathol Exp Neurol *68*, 736-746.

Gu, X., Olson, E.C., and Spitzer, N.C. (1994). Spontaneous neuronal calcium spikes and waves during early differentiation. J Neurosci *14*, 6325-6335.

Gu, X., and Spitzer, N.C. (1993). Low-threshold Ca2+ current and its role in spontaneous elevations of intracellular Ca2+ in developing Xenopus neurons. J Neurosci *13*, 4936-4948.

Hamburger, V. (1975). Cell death in the development of the lateral motor column of the chick embryo. J Comp Neurol *160*, 535-546.

Hamburger, V., and Yip, J.W. (1984). Reduction of experimentally induced neuronal death in spinal ganglia of the chick embryo by nerve growth factor. J Neurosci *4*, 767-774.

Hanson, M.G., and Landmesser, L.T. (2004). Normal patterns of spontaneous activity are required for correct motor axon guidance and the expression of specific guidance molecules. Neuron *43*, 687-701.

Hanson, M.G., Milner, L.D., and Landmesser, L.T. (2008). Spontaneous rhythmic activity in early chick spinal cord influences distinct motor axon pathfinding decisions. Brain Res Rev *57*, 77-85.

Herzog, R.I., Cummins, T.R., and Waxman, S.G. (2001). Persistent TTX-resistant Na+ current affects resting potential and response to depolarization in simulated spinal sensory neurons. J Neurophysiol *86*, 1351-1364.

Holliday, J., and Spitzer, N.C. (1990). Spontaneous calcium influx and its roles in differentiation of spinal neurons in culture. Dev Biol *141*, 13-23.

Huang, X., Huang, P., Robinson, M.K., Stern, M.J., and Jin, Y. (2003). UNC-71, a disintegrin and metalloprotease (ADAM) protein, regulates motor axon guidance and sex myoblast migration in C. elegans. Development *130*, 3147-3161.

Hughes, R.A., and O'Leary, P.D. (1996). Neurotrophic factors and the development of drugs to promote motoneuron survival. Clin Exp Pharmacol Physiol *23*, 965-969.

Jablonka, S., Beck, M., Lechner, B.D., Mayer, C., and Sendtner, M. (2007).
Defective Ca2+ channel clustering in axon terminals disturbs excitability in motoneurons in spinal muscular atrophy. J Cell Biol *179*, 139-149.

Kafitz, K.W., Rose, C.R., Thoenen, H., and Konnerth, A. (1999). Neurotrophin-evoked rapid excitation through TrkB receptors. Nature *401*, 918-921.

Kaiser, P.K., and Lipton, S.A. (1990). VIP-mediated increase in cAMP prevents
tetrodotoxin-induced retinal ganglion cell death in vitro. Neuron *5*, 373-381.

Krafte, D.S., and Bannon, A.W. (2008). Sodium channels and nociception: recent concepts and therapeutic opportunities. Curr Opin Pharmacol *8*, 50-56.

Kuczewski, N., Porcher, C., Lessmann, V., Medina, I., and Gaiarsa, J.L. (2009). Activity-dependent dendritic release of BDNF and biological consequences. Mol Neurobiol *39*, 37-49.

Landmesser, L.T., and O'Donovan, M.J. (1984). Activation patterns of embryonic chick hind limb muscles recorded in ovo and in an isolated spinal cord preparation. J Physiol *347*, 189-204.

Lang, S.B., Stein, V., Bonhoeffer, T., and Lohmann, C. (2007). Endogenous brain-derived neurotrophic factor triggers fast calcium transients at synapses in developing dendrites. Journal of Neuroscience *27*, 1097-1105.

Lefebvre, J.L., Ono, F., Puglielli, C., Seidner, G., Franzini-Armstrong, C., Brehm, P., and Granato, M. (2004). Increased neuromuscular activity causes axonal defects and muscular degeneration. Development *131*, 2605-2618.

Leo, S., D'Hooge, R., and Meert, T. (2010). Exploring the role of nociceptor-specific sodium channels in pain transmission using Nav1.8 and Nav1.9 knockout mice. Behav Brain Res *208*, 149-157.

Lewis, K.E., and Eisen, J.S. (2003). From cells to circuits: development of the zebrafish spinal cord. Prog Neurobiol *69*, 419-449.

Lipton, S.A. (1986). Blockade of electrical activity promotes the death of mammalian retinal ganglion cells in culture. Proc Natl Acad Sci U S A *83*, 9774-9778.

Meister, M., Wong, R.O., Baylor, D.A., and Shatz, C.J. (1991). Synchronous bursts of action potentials in ganglion cells of the developing mammalian retina. Science *252*, 939-943.

Mennerick, S., and Zorumski, C.F. (2000). Neural activity and survival in the developing nervous system. Mol Neurobiol *22*, 41-54.

Metzger, F., Kulik, A., Sendtner, M., and Ballanyi, K. (2000). Contribution of Ca(2+)-permeable AMPA/KA receptors to glutamate-induced Ca(2+) rise in embryonic lumbar motoneurons in situ. J Neurophysiol *83*, 50-59.

Milner, L.D., and Landmesser, L.T. (1999). Cholinergic and GABAergic inputs drive patterned spontaneous motoneuron activity before target contact. J Neurosci *19*, 3007-3022.

Ming, G., Henley, J., Tessier-Lavigne, M., Song, H., and Poo, M. (2001). Electrical activity modulates growth cone guidance by diffusible factors. Neuron *29*, 441-452.

Monani, U.R., Sendtner, M., Coovert, D.D., Parsons, D.W., Andreassi, C., Le, T.T., Jablonka, S., Schrank, B., Rossoll, W., Prior, T.W*., et al.* (2000). The human centromeric survival motor neuron gene (SMN2) rescues embryonic lethality in Smn(-/-) mice and results in a mouse with spinal muscular atrophy. Hum Mol Genet *9*, 333-339.

Moody, W.J., and Bosma, M.M. (2005). Ion channel development, spontaneous activity, and activity-dependent development in nerve and muscle cells. Physiol Rev *85*, 883-941.

Murray, L.M., Comley, L.H., Thomson, D., Parkinson, N., Talbot, K., and Gillingwater, T.H. (2008). Selective vulnerability of motor neurons and dissociation of pre- and post-synaptic pathology at the neuromuscular junction in mouse models of spinal muscular atrophy. Hum Mol Genet *17*, 949-962.

Naldini, L., Blomer, U., Gage, F.H., Trono, D., and Verma, I.M. (1996). Efficient transfer, integration, and sustained long-term expression of the transgene in
adult rat brains injected with a lentiviral vector. Proc Natl Acad Sci U S A *93*, 11382-11388.

Nishimaru, H., Iizuka, M., Ozaki, S., and Kudo, N. (1996). Spontaneous motoneuronal activity mediated by glycine and GABA in the spinal cord of rat fetuses in vitro. J Physiol *497 (Pt 1)*, 131-143.

O'Donovan, M.J., Chub, N., and Wenner, P. (1998). Mechanisms of spontaneous activity in developing spinal networks. J Neurobiol *37*, 131-145.

Ostman, J.A., Nassar, M.A., Wood, J.N., and Baker, M.D. (2008). GTP up-
regulated persistent Na+ current and enhanced nociceptor excitability require NaV1.9. J Physiol *586*, 1077-1087.

Penzotti, J.L., Fozzard, H.A., Lipkind, G.M., and Dudley, S.C., Jr. (1998). Differences in saxitoxin and tetrodotoxin binding revealed by mutagenesis of the Na+ channel outer vestibule. Biophys J *75*, 2647-2657.

Provine, R.R. (1972). Ontogeny of bioelectric activity in the spinal cord of the chick embryo and its behavioral implications. Brain Res *41*, 365-378.

Ren, J., and Greer, J.J. (2003). Ontogeny of rhythmic motor patterns generated in the embryonic rat spinal cord. J Neurophysiol *89*, 1187-1195.

Rossoll, W., Jablonka, S., Andreassi, C., Kroning, A.K., Karle, K., Monani, U.R., and Sendtner, M. (2003). Smn, the spinal muscular atrophy-determining gene product, modulates axon growth and localization of beta-actin mRNA in growth cones of motoneurons. J Cell Biol *163*, 801-812.

Rubinson, D.A., Dillon, C.P., Kwiatkowski, A.V., Sievers, C., Yang, L., Kopinja, J., Rooney, D.L., Zhang, M., Ihrig, M.M., McManus, M.T.*, et al.* (2003). A lentivirus-based system to functionally silence genes in primary mammalian cells, stem cells and transgenic mice by RNA interference. Nat Genet *33*, 401-406.

Rugiero, F., Mistry, M., Sage, D., Black, J.A., Waxman, S.G., Crest, M., Clerc, N., Delmas, P., and Gola, M. (2003). Selective expression of a persistent tetrodotoxin-resistant Na+ current and NaV1.9 subunit in myenteric sensory neurons. J Neurosci *23*, 2715-2725.

Rush, A.M., and Waxman, S.G. (2004). PGE2 increases the tetrodotoxin-resistant Nav1.9 sodium current in mouse DRG neurons via G-proteins. Brain Res *1023*, 264-271.

Sanes, J.R., and Lichtman, J.W. (1999). Development of the vertebrate neuromuscular junction. Annu Rev Neurosci *22*, 389-442.

Schmalbruch, H., Jensen, H.J., Bjaerg, M., Kamieniecka, Z., and Kurland, L. (1991). A new mouse mutant with progressive motor neuronopathy. J Neuropathol Exp Neurol *50*, 192-204.

Schmidt, E.R., Pasterkamp, R.J., and van den Berg, L.H. (2009). Axon guidance proteins: novel therapeutic targets for ALS? Prog Neurobiol *88*, 286-301.

Schneider, V.A., and Granato, M. (2003). Motor axon migration: a long way to go. Dev Biol *263*, 1-11.

Sendtner, M. (2001). Molecular mechanisms in spinal muscular atrophy: models and perspectives. Curr Opin Neurol *14*, 629-634.

Sendtner, M., Pei, G., Beck, M., Schweizer, U., and Wiese, S. (2000). Developmental motoneuron cell death and neurotrophic factors. Cell Tissue Res *301*, 71-84.

Sivilotti, L., Okuse, K., Akopian, A.N., Moss, S., and Wood, J.N. (1997). A single serine residue confers tetrodotoxin insensitivity on the rat sensory-neuron-specific sodium channel SNS. FEBS Lett *409*, 49-52.

Son, J.H., and Winzer-Serhan, U.H. (2009). Chronic neonatal nicotine exposure increases mRNA expression of neurotrophic factors in the postnatal rat hippocampus. Brain Res *1278*, 1-14.

Spitzer, N.C. (2006). Electrical activity in early neuronal development. Nature *444*, 707-712.

Spitzer, N.C., Debaca, R.C., Allen, K.A., and Holliday, J. (1993). Calcium dependence of differentiation of GABA immunoreactivity in spinal neurons. J Comp Neurol *337*, 168-175.

Spitzer, N.C., Olson, E., and Gu, X. (1995). Spontaneous calcium transients regulate neuronal plasticity in developing neurons. J Neurobiol *26*, 316-324.

Spitzer, N.C., and Ribera, A.B. (1998). Development of electrical excitability in embryonic neurons: mechanisms and roles. J Neurobiol *37*, 190-197.

Takahashi, K., and Okamura, Y. (1998). Ion channels and early development of neural cells. Physiol Rev *78*, 307-337.

Thoenen, H. (2000). Neurotrophins and activity-dependent plasticity. Prog Brain Res *128*, 183-191.

Wiese, S., Herrmann, T., Drepper, C., Jablonka, S., Funk, N., Klausmeyer, A., Rogers, M.L., Rush, R., and Sendtner, M. (2010). Isolation and enrichment of embryonic mouse motoneurons from the lumbar spinal cord of individual mouse embryos. Nat Protoc *5*, 31-38.

Wood, J.N., Abrahamsen, B., Baker, M.D., Boorman, J.D., Donier, E., Drew, L.J., Nassar, M.A., Okuse, K., Seereeram, A., Stirling, C.L.*, et al.* (2004a). Ion channel activities implicated in pathological pain. Novartis Found Symp *261*, 32-40; discussion 40-54.

Wood, J.N., Boorman, J.P., Okuse, K., and Baker, M.D. (2004b). Voltage-gated sodium channels and pain pathways. J Neurobiol *61*, 55-71.

Yuste, R., Peinado, A., and Katz, L.C. (1992). Neuronal domains in developing neocortex. Science *257*, 665-669.

Yvert, B., Branchereau, P., and Meyrand, P. (2004). Multiple spontaneous rhythmic activity patterns generated by the embryonic mouse spinal cord occur within a specific developmental time window. J Neurophysiol *91*, 2101-2109.

Zheng, J.Q., and Poo, M.M. (2007). Calcium signalling in neuronal motility. Annu Rev Cell Dev Biol *23*, 375-404.

8. List of figures and tables

List of tables

9. Abbreviations

ACSF	artificial cerebrospinal fluid
ALS	Amyotrophic lateral sclerosis
ATP	adenosine triphosphate
BDNF	Brain Derived Neurotrophic Factor
CsCl	cesium chloride
CMV	Cytomegalovirus
CNTF	Ciliary Neurotrophic Factor
cDNA	complementary DNA
dNTP	deoxynucleotide triphosphate
°C	centigrade Celsius
DAPI	4', 6-diamidino-2-phenylindole
DEPC	Diethylpyrocarbonate
dd H_2O	doubled distilled water
DIV	days in vitro
DMSO	Dimethyl sulphoxide
DNA	deoxyribonucleic acid
E.coli	*Escherichia coli*
EDTA	Ethylenediaminetetraacetic acid
eGFP	enhanced GFP
EtBr	ethidium bromide
FCS	fetal calf serum
FITC	Fluorescein isothiocyanate
fwd	forward
G418	Geneticin
GDNF	Glial cell derived neurotrophic factor
GFP	green fluorescent protein
HBSS	Hank's balanced salt solution
HEK 293	Human embryonic kidney cells 293
hrs	hours
IgG	Immunoglobulin G
IGF	insulin like growth factor

ko	knock out
LB	Luria Bertani
LIF	leukaemia inhibitory factor
mRNA	messenger RNA
mg	milligram
min	minute
mM	millimolar
µ	micro
µg	microgram
µM	micromolar
nM	nanomolar
NGF	nerve growth factor
NT	neurotrophin
NVT	Near vertical titanium (Beckman rotors)
PBS	phosphate buffer saline
PCR	polymerase chain reaction
PFA	paraformaldehyde
rev	reverse
RFP	red fluorescent protein
RRE	Rev-responsive element
RSV	Rous sarcoma virus
RNA	ribonucleic acid
RT-PCR	reverse transcription PCR
s	seconds
SOB	super optimal broth
SOC	super optimal broth with catabolite repression.
SEM	standard Error of Mean
SMA	Spinal Muscular Atrophy
shRNA	short hairpin RNA
STX	saxitoxin
TE	Tris EDTA
Trk	Tropomyosin-related-kinase

TTX	tetrodotoxin
VSVG	Vesicular stomatitis virus
VGCC	voltage-gated calcium channels
VGSC	voltage-gated sodium channels
wt	wild-type

10. Declaration

I hereby declare that the work presented here was performed by me and none other. All the materials and resources that have been utilized in this work are solely enclosed in this thesis. I also declare that the following dissertation entitled, “Role of $Na_v1.9$ in activity dependent axon growth in embryonic cultured motoneurons” has not been submitted earlier and has not been used for obtaining any other equivalent qualification in any other organization. Additionally, other than this degree I have not applied or will not attempt to apply for any other degree, title or qualification in relation to this work.

Narayan Subramanian

Publications:

1. Role of $Na_v1.9$ in activity dependent axon growth in motoneurons. Narayan Subramanian, Benjamin Dombert, Andrea Wetzel, Steven Havlicek, Sibylle Jablonka, Mohammed A. Nassar, Robert Blum[1] & Michael Sendtner[1] (Manuscript submitted). [1] equal contribution

2. Drosophila KAP interacts with the kinesin II motor subunit KLP64D to assemble chordotonal sensory cilia, but not sperm tails. **Current Biology 13, 1687-1696**. Sarpal, R., Todi, S.V., Sivan-Loukianova, E., Shirolikar, S., **Subramanian, N**., Raff, E.C., Erickson, J.W., Ray, K., and Eberl, D.F. (2003).

Acknowledgements

I am very glad to have gone on this through this Ph.D. journey and firmly believe in the omnipresent God, for answering my prayers and giving me the strength to plod through every step of this journey. This dissertation work has been made possible with the guidance and help of several individuals who in one way or another contributed and have extended their valuable assistance in the preparation and completion of this study.

I thank my supervisor, Prof. Dr. Michael Sendtner, for providing me an esteemed opportunity to work under his guidance and encouraged me to learn the finest principles of scientific research. I am immensely grateful for his valuable and uninterrupted financial support throughout my PhD tenure. I also highly appreciate his complete support in allowing me to present my work in international scientific conferences.

I am indebted to PD. Dr Robert Blum for his valuable guidance towards my project right from the day he joined the department. His unbiased critical attention to details and contagious work ethics will always be a valuable learning experience. I am immensely grateful to him for sharing his expertise and teaching the nitty-gritty's of all the scientific experiments in this project. A journey is easier when you travel together; Interdependence is certainly more valuable than independence.

I thank Regine Sendtner, Helga Brunner, J.Horschig and V.Buterus for their assistance in maintaining and availing the laboratory animals to carry out my experiments. Their undying patience to bear my broken German language has been commendable quality. I also would like to thank the technical staff, Katrin, Sonja, Nicole, Christina, Zuzana, Michi, Simone, Elke and Hilde for their valuable support and co-operation. I would also like to thank Judita Grimm, Urveen Oberoi- Lehrieder and Christ Birgit for their administrative assistance.

The days of my research work starting from the kopfklinik to MSZ in Würzburg, has been an wonderful experience and I am happy to be one among

the vast work group of Prof. M. Sendtner. I thank all colleagues for the extensive co-operative, interactive and for a stimulating fun-filled environment. This includes Andrea Wetzel, Andreska Thomas, Benjamin Dombert, Bhuvaneish Selvaraj, Carsten Drepper, Chandrakanth Reddy, Christian Simon, Christina Mais, Dirk Pühringer, Elena Nekhorhoshkova, Florian Bender, Frank Krieger, Juliane Jäpel, Lena Saal, Lidia Albanito, Michael Glinka, Nadya Orel, Natalya Funk, Nicholas Frank, PD Dr. Sibylle Jablonka, PD. Dr. Rudolf Götz, Preeti Yadav, Prof. Dr.Anna Maria Musti, Rajeeve Sivadasan, Reena Rathod, Sameehan Mahajani, Stephan Weise, Steven Havlicek, Thomas Hermann and Wilfred Rossoll.

I would like to extend my sincere thanks to the funding agencies that supported my work:
BIGSS – BioMedTec International Graduate School of Science,
Deutsche Forschungsgemeinschaft, BL567 and SFB581- project B1 and B24 and the from the Hermann und Lilly Schilling Stiftung im Stifterverband der Deutschen Wissenschaft.

My family is an important part of my life and I am extremely grateful for their love and encouragements throughout my PhD tenure. I thank my parents for their unconditional support in all the decisions of my life and I owe them my sincere gratitude for being my pillars of strength and a virtual backbone throughout this work. I also thank my parents-in- law, who have always encouraged me and provided moral support. The unconditional love, care, patience and sacrifices showered by my wife, Sowmya, is priceless. I will always be indebted to her for keeping me constantly motivated during happy and hard moments. It's difficult not to mention my nine month old Sarvesh. Since his birth, he has reignited my enthusiasm in life and always kept me in high spirits towards the finals stages of my PhD tenure. .

Life in Würzburg would have been meaningless without the presence of my friends. A special thanks to all of them for colouring my life and being there during all the good and the bad roller coaster rides. I also owe it to this wonderful city for making my stay here memorable.